

XINSIGHT: eXplainable Data Analysis Through The Lens of Causality

Pingchuan Ma

HKUST

Hong Kong SAR, China

pmaab@cse.ust.hk

Rui Ding

Microsoft Research

Beijing, China

juding@microsoft.com

Shuai Wang

HKUST

Hong Kong SAR, China

shuaiw@cse.ust.hk

Shi Han

Microsoft Research

Beijing, China

Dongmei Zhang

Microsoft Research

Beijing, China

ABSTRACT

In light of the growing popularity of Exploratory Data Analysis (EDA), understanding the underlying causes of the knowledge acquired by EDA is crucial, but remains under-researched. This study promotes for the first time a transparent and explicable perspective on data analysis, called *eXplainable Data Analysis* (XDA). XDA provides data analysis with qualitative and quantitative explanations of causal and non-causal semantics. This way, XDA will significantly improve human understanding and confidence in the outcomes of data analysis, facilitating accurate data interpretation and decision making in the real world. For this purpose, we present XINSIGHT, a general framework for XDA. XINSIGHT is a three-module, end-to-end pipeline designed to extract causal graphs, translate causal primitives into XDA semantics, and quantify the quantitative contribution of each explanation to a data fact. XINSIGHT uses a set of design concepts and optimizations to address the inherent difficulties associated with integrating causality into XDA. Experiments on synthetic and real-world datasets as well as human evaluations demonstrate the highly promising capabilities of XINSIGHT.

PVLDB Artifact Availability:

The source code, data, and/or other artifacts have been made available at URL_TO_YOUR_ARTIFACTS.

1 INTRODUCTION

Exploratory data analysis (EDA) is a key step for acquiring insight from data and facilitating analysis towards decision making [25, 33]. With the advent of the digital age, the information explosion phenomenon [10] makes it difficult for users to justify and rely on knowledge and conclusions from EDA. To ease the cognitive process, data explanations are proposed to deliberate data facts (e.g., query outcomes) and enhance user comprehension [17]. In this paper, we advocate such process as *eXplainable Data Analysis* (XDA), which advances data analysis by providing users with effective explanations. XDA aids users in understanding and trusting phenomena surfaced from data, by suggesting and justifying choices to alter outcomes; as a result, it facilitates real-world decision making.

Explanations are classified as either causal or non-causal [21]. Causal explanations seek causal factors to explain an outcome. Consider Fig. 1, which contains a hypothetical lung cancer dataset. Here, a patient’s location influences (by local tobacco control policy) whether he/she will smoke, and the patient’s stress level also

affects smoking. Consequently, smoking affects the severity of lung cancer. The severity determines whether the patient will undergo surgery and his/her five-year survival rate. In this case, smoking explains why a patient had high lung cancer severity (see Fig. 1(f)). In contrast, a non-causal explanation works by showing the result to be mere statistical correlations. For example, surgery “explains” (or, more precisely, is relevant to) lung cancer severity (see Fig. 1(g)). It is useful in retrospect, but should be a non-causal explanation [40].

Most existing data explanation tools (e.g., Scorpion [49] and DIFF [3] in academia and Tableau’s Explain Data [2] in industry) provide non-causal explanations [17]. While valuable for data analysis, they may confuse or mislead users who demand causal explanations. According to [22], Tableau’s Explain Data reports that Massachusetts’ low teen pregnancy rate may explain this state’s high ACT Math score. Such explanations are questionable. In comparison, causal explanations play a central role in human cognition [20, 34]. They enable users to make counterfactual thinking and actionable decisions. For instance, giving up smoking lowers the severity of lung cancer while avoiding a surgery does not.

Causal knowledge is typically represented in the form of causal graphs, according to Pearl’s general causality [35]. Given a causal graph, each node represents a random variable in the data and each directed edge indicates a cause-effect relation between the parent and child nodes. Causal knowledge primarily conveys *qualitative explanations* [45], e.g., smoking causes lung cancer. To further enable *quantitative explanations*, one needs to quantify each input’s contribution to the outcome. This way, we can measure smoking’s contribution to lung cancer and compare it to other factors. Quantitative explanations can be elegantly formulated by Halpern’s actual causality [18, 19], particularly by its adaption called DB Causality referred to by the database community [28].

This paper proposes XINSIGHT as a unified, causality-based framework for XDA. Given a dataset (as in Fig. 1(a)), a user observes an interesting data fact and then raises a WHY QUERY, as in Fig. 1(b). XINSIGHT outputs a set of explanations (see Fig. 1(f) and (g)). Each explanation conveys whether it is a causal or non-causal explanation, and is composed with both qualitative and quantitative sub-explanations. For instance, XINSIGHT considers “Smoking” as a causal factor of lung cancer severity and highlights “Smoking=Yes” and its responsibility as a quantitative sub-explanation.

XINSIGHT includes three modules, XLEARNER, XTRANSLATOR, and XPLAINERS to gradually form explanations. XLEARNER first automatically discovers a causal graph G from data (Fig. 1(c)). Then,

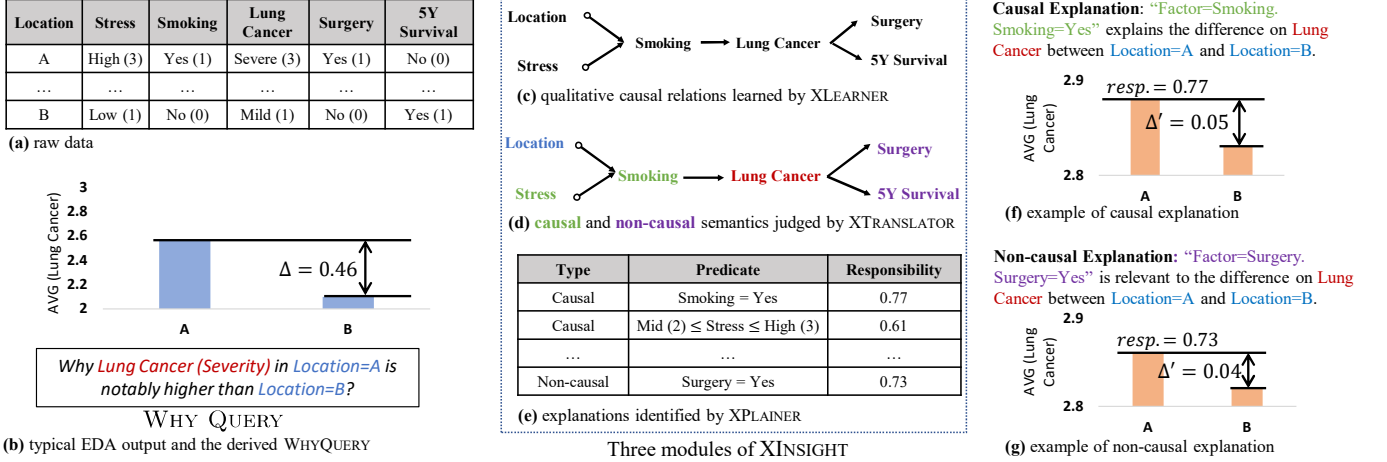


Figure 1: Illustrative example of XINSIGHT.

given a WHY QUERY with the target (i.e., “Lung Cancer”) and the context (i.e., “Location”), XTRANSLATOR enumerates each remaining variable on G and decides if it is causal or non-causal to the target under the context. Fig. 1(d) shows causal variables (i.e., can potentially provide causal explanations) in green and non-causal variables (i.e., can potentially provide non-causal explanations) in purple. Last, XPLAINER quantifies how well each variable answers WHY QUERY by searching possible predicates on the variable that are the most responsible, as shown in Fig. 1(e). Despite the promising capability of XINSIGHT, concretizing each module is challenging.

XLEARNER. Most real-world datasets are collected irrespective of causal sufficiency [38]. In words, not all causally relevant variables are available in the dataset. On the other hand, real-world datasets often contain deterministic relations in the form of Functional Dependency (FD), especially when materialized from relational databases. These FDs may violate faithfulness assumption [14], which are crucial for many causal discovery algorithms. To address these challenges, we establish a theory to propose an FD-induced graph G_{FD} . XLEARNER use G_{FD} to select a subset of variables for standard causal discovery where the selected variables would not trigger faithfulness violations. It adopts FCI [52] to address causal insufficiency and synergistically combine the result of FCI with causal relations entailed by G_{FD} .

XTRANSLATOR. The translation from causal primitives into XDA semantics (e.g., whether a variable provides causal explanations or has no explanation power) is under-explored. Given a WHY QUERY (with a target and a context), it is unclear how to determine if X can explain the target given the context and, more importantly, if X provides causal or non-causal explanations. XTRANSLATOR characterizes various causal primitives (e.g., m-separation, ancestor/descendant relations) from a causal graph and provides a systematic way to translates them into XDA semantics.

XPLAINER. DB causality is primarily designed for data provenance, which usually provides tuples as explanations. Contrarily, predicate-level explanations are more desirable for XDA scenarios. Moreover, computing the responsibility of explanations with DB causality is NP-complete in general [29]. XPLAINER adapts DB causality to XDA

by using predicate-level explanation with conciseness consideration and significantly reduces the computing cost with theoretical guarantees. In summary, we make the following contributions:

- We advocate a novel, important, and general enhancement over EDA, namely *eXplainable data analysis* (XDA). XDA principally delivers effective explanations to engage users with data insights towards real-world decision making. In words, XDA makes data analysis more credible and practical.
- Our proposed framework, XINSIGHT, features adequate (by distinguishing causal vs. non-causal) and comprehensive (with both qualitative and quantitative) explanations. XINSIGHT consists of three modules, XLEARNER, XTRANSLATOR and XPLAINER, each of which is meticulously designed to address technical challenges and deliver efficient analysis.
- Empirically, we conduct thorough experiments on the public data, production data, and synthetic data via quantitative experiments and human evaluations. The results are highly encouraging.

Open Source and Real-world Adoption. We have uploaded an artifact and will release the code after undergoing an internal review. We also maintain an extended version of the paper (including Supplementary Material) on arXiv [26]. XPLAINER is now integrated into Explain Increase/Decrease feature of Microsoft Power BI [1].

2 PRELIMINARY

2.1 Data Model and Query

Multi-dimensional Data. Let $D := \{X_1, \dots, X_n\}$ represent a multi-dimensional data consisting n attributes. In XINSIGHT, we assume records of D are sampled from an independent and identical distribution such that each attribute can be viewed as a (random) variable. A variable is either categorical or numerical. Following the conventions in data analysis [13, 25], we denote a categorical variable as *dimension* and a numerical variable as *measure*. For relational data, we anticipate to take a materialized provenance table [23] as the input to our system.

Aggregation and Discretization on Measure. Given a measure M , users may perform aggregation operations (such as SUM and

AVG in SQL) over a set of realizations of M . In some cases, users may anticipate to process measures in the form of a dimension (e.g., use measures for explanations), which necessitates discretization. Discretization transforms numerical values into several discrete bins that form a categorical variable.

Filter. In XINSIGHT, filter is the basic unit of data operations. Given a multi-dimensional data D and a dimension X , a filter $p_i = \{X = x_i\}$ (e.g., “Smoking=Yes”) implies an equality assertion to X such that the value on X shall equal x_i .

Predicate. A predicate is the disjunction of filters applied to the same dimension. Given the dimension X , the predicate $P(x_1, \dots, x_k)$ is a set containment assertion $\{X = x_1 \vee \dots \vee X = x_k\} \equiv \{p_1, \dots, p_k\}$. On a discretized measure, a predicate is an assertion on ranges. A filter is a special case of a predicate. For clarity, we represent a general predicate by upper-case P and a filter by lower-case p .

Subspace. A subspace is the conjunction of filters on disjoint dimensions. Given multi-dimensional data D , the subspace corresponds to a subset of rows satisfying the conditions of all filters. For instance, $s = \{\text{Location} = \text{A} \wedge \text{Lung Cancer} = \text{Severe}\}$ represents the subspace denoting all patients in “Location=A” with severe lung cancer. Two subspaces are considered *siblings* if they differ in only a single filter (e.g., all patients in “Location=A” with severe lung cancer v.s. all patients in “Location=B” with severe lung cancer). *Context* refers to the variables associated with two sibling subspaces, where variables associated with the shared filters are called *background variables*, and the variable associated with a different filter is called the *foreground variable*. In the preceding example, “Location” is the foreground variable and “Lung Cancer” is the background variable. **Selection.** We use the following notation to denote the selection operation over multi-dimensional data D . The subset of data after selection operation is defined as D_{p_i} , D_P or D_s , where p_i is a filter, P is a predicate and s is a subspace. We also define $D - D'$ as the rows in D after removing the rows in D' . In addition, we also denote $D - P$ as an abbreviation for $D - D_P$.

WHY QUERY and Explanation. Explaining the distinction between two aggregate queries is one prevalent data analysis task. Identifying the cause of data difference facilitates many data explanation applications, such as outlier explanation and data debugging [17]. In this research, we concretize the problem of XDA by focusing on the explanation of *data difference*, as has been the case in many earlier works [3, 17, 49]. We define WHY QUERY as follows.

DEFINITION 2.1 (WHY QUERY). *Given a multi-dimensional data D , a user launches aggregate query $\text{agg}()$ on a target measure M under two sibling subspaces s_1, s_2 . WHY QUERY is defined as $\Delta_{s_1, s_2, M, \text{agg}}(D) = \text{agg}_M(D_{s_1}) - \text{agg}_M(D_{s_2})$. For brevity, we use $\Delta(D)$ as the shorthand of $\Delta_{s_1, s_2, M, \text{agg}}(D)$.*¹

Recalling the example in Fig. 1(b), we concretize the WHY QUERY Δ with an average aggregation on the target “Lung Cancer” over two sibling subspaces $s_1 = \{\text{Location} = \text{A}\}$ and $s_2 = \{\text{Location} = \text{B}\}$, which can be interpreted as the average lung cancer severity in “A” and “B”. This query formulates users’ curiosity about the difference Δ of lung cancer severity between the two locations, where “Lung Cancer” forms the target in WHY QUERY and “Location” forms the

context. Upon receiving this WHY QUERY, we intend to identify explanations for Δ in the following format.

DEFINITION 2.2 (EXPLANATION). *Given a WHY QUERY, an explanation is represented by the following triplet*

$$\text{explanation} := \langle \text{type}, \text{predicate}, \text{responsibility} \rangle \quad (1)$$

where $\text{type} \in \{\text{causal, non-causal}\}$ denotes whether the explanation is causal or non-causal, predicate is the content of the explanation, and responsibility , a score ranging from 0 to 1, quantifies the extent to which the explanation explains the given WHY QUERY.

We list several examples of explanations in Fig. 1(e). The explanation in Fig. 1(g) is a non-causal explanation and depicts that “Surgery=Yes” is relevant to the lung cancer severity difference.

Functional Dependency (FD). Functional dependency relations are common in multi-dimensional data. Typically, in a relational database, there may exist primary keys and foreign keys among attributes. Therefore, after materialization, the resulting multi-dimensional data may have functional dependencies. A functional dependency between X and Y is represented by $X \xrightarrow{\text{FD}} Y$ (e.g., city $\xrightarrow{\text{FD}} \text{country}$). FD can be viewed as a form of deterministic knowledge about the data, typically more reliable than a stochastic relation (e.g., the general form of causal relations) between two variables. This research focuses on one-to-one and one-to-many FDs.

FD-Induced Graph. Given a multi-dimensional data D and its functional dependencies, the FD-induced Graph $G_{\text{FD}} := (V, E)$, where $V := \{A_i \mid \forall A_i \in D\}$ and $E := \{(A_i, A_j) \mid \text{if } A_i \xrightarrow{\text{FD}} A_j\}$. We assume G_{FD} to be acyclic. Cycles in G_{FD} imply redundant attributes; in such cases, we retain only one of them to ensure acyclicity.

2.2 Causal Discovery

This section presents terminology essential to causal discovery, such as the representation of causal graphs under causal insufficiency and typical assumptions in causal discovery.

Table 1: Four types of edges in PAG.

Edge	Causal Semantics
$X \rightarrow Y$	X is a cause of Y .
$X \leftrightarrow Y$	X and Y share a latent common cause.
$X \circ \rightarrow Y$	1) X may be a cause of Y or 2) X and Y share a latent common cause.
$X \circ \circ Y$	1) X may be a cause of Y or 2) Y may be a cause of X . or 3) X and Y share a latent common cause.

MAG and PAG. Maximal Ancestral Graph (MAG) is a well-established representation of causal graphs under causal insufficiency. Typically, it contains two types of edges (the first two edges in Table 1). Let a MAG G be the ground-truth causal graph. Causal discovery algorithms can recover the Markov equivalence class of G , called Partial Ancestral Graph (PAG), which has four types of edges, from the data (see Table 1). Markov equivalence class denotes a set of MAGs that are compatible with the same data. In that sense, PAG contains edges of uncertain directions (the last two edges in Table 1), indicating that this direction is unidentifiable and either direction fits the data equally well. We refer readers to [52] for a rigorous definition. We now introduce additional terminology and assumptions used in our work.

¹Without loss of generality, we assume Δ is always non-negative.

DEFINITION 2.3 (M-SEPARATION [52]). In a PAG, a path p between X, Y is active relative to Z if (1) every non-collider on p is not a member of Z and (2) every collider on p has a descendant in Z .² X, Y are m-separated by Z ($X \perp\!\!\!\perp_G Y \mid Z$) if there does not exist an active path p between X, Y relative to Z .

Faithfulness and Global Markov Property. m-separation is a structural constraint over a causal graph. The faithfulness assumption allows us to deduce such constraints according to statistical relations from data and gradually form a causal graph. Formally, it implies the following Eqn. 2.

$$X \perp\!\!\!\perp Y \mid Z \Rightarrow X \perp\!\!\!\perp_G Y \mid Z \quad (2)$$

With the faithfulness assumption, causal discovery algorithms can conduct statistical hypothesis tests for conditional independence in data and then infer causal relations on the causal graph. In contrast to faithfulness assumption, Global Markov Property (GMP) reverses Eqn. 2. It entails that if X, Y are m-separated by Z , then X, Y are conditionally independent given Z in the data. Formally, $X \perp\!\!\!\perp_G Y \mid Z \Rightarrow X \perp\!\!\!\perp Y \mid Z$.

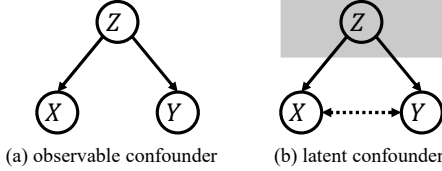


Figure 2: Examples of observable and latent confounders.

Causal Sufficiency. The absence of unmeasured confounders is commonly assumed in causal discovery algorithms. “Confounders” (Z in Fig. 2) refer to the common causes of two variables (X, Y in Fig. 2), and the assumption implies that all confounders are observed in the data. Hence, if Z is observed in the data (Fig. 2(a)), there would be no spurious edge between X, Y . Nevertheless, if Z is not observed (thus $Z \rightarrow X$ and $Z \rightarrow Y$ cannot be identified), there would be a spurious association between X, Y [36].

3 XINSIGHT

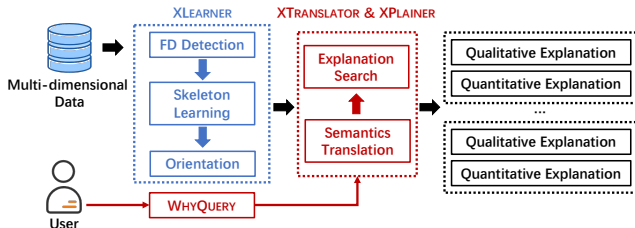


Figure 3: Workflow of XINSIGHT.

XINSIGHT delivers a unified framework for explainable data analysis with three modules. The workflow of XINSIGHT is shown in Fig. 3. First, given a multi-dimensional data D , XLEARNER pre-learns

²A node T is called a collider on p if $A \rightarrow T \leftarrow B$, $A \rightarrow T \leftarrow B$, $A \rightarrow T \leftarrow B$, or $A \rightarrow T \leftarrow B$.

a causal graph G from data in the offline phase (blue-annotated in Fig. 3). Then, in the online phase (red-annotated in Fig. 3), upon receiving a WHY QUERY, XTRANSLATOR identifies variables that have potentials to give either causal or non-causal explanations based on the causal primitives on G . Finally, XPLAINER examines each identified variable with potentials and decides the optimal explanation for the given WHY QUERY. After applying XPLAINER to all variables with potentials, XINSIGHT yields a set of explanations (with qualitative sub-explanation and quantitative sub-explanation). By decoupling XINSIGHT into an offline phase and an online phase, heavy-weight computations are performed beforehand, and only light-weight computations are needed in the online phase, allowing for a rapid response to a user’s query. In the following, we elaborate on the design of each module. Due to page limits, we present proofs and theoretical discussion in Supplementary Material [26].

3.1 XLEARNER

As noted in Sec. 2.2, it is hard to guarantee causal sufficiency for real-world data. Therefore, XLEARNER aims to learn a PAG from data. Moreover, in the presence of functional dependencies (FD), faithfulness can be easily violated [14]. In the following, we show how FD would impose violations of the faithfulness assumption.

Considering a simple case where $X \xrightarrow{\text{FD}} Y \xrightarrow{\text{FD}} Z$ (e.g., X is city, Y is state, and Z is country), we have $X \xrightarrow{\text{FD}} Y$, $Y \xrightarrow{\text{FD}} Z$, and $X \xrightarrow{\text{FD}} Z$. Then, we have $Y \perp\!\!\!\perp Z \mid X$ and $X \perp\!\!\!\perp Z \mid Y$. If faithfulness assumption holds, we can imply that $Y \perp\!\!\!\perp_G Z \mid X$ and $X \perp\!\!\!\perp_G Z \mid Y$. Therefore, Z is non-adjacent to both X and Y and we have $Y \perp\!\!\!\perp_G Z$. By GMP, we can imply that $Y \perp\!\!\!\perp Z$, which contradicts functional dependencies on $Y \xrightarrow{\text{FD}} Z$. Thus, if we directly apply standard causal discovery algorithms on variables with FD, we cannot obtain correct causal relationships from data.

Table 2: Comparing different causal discovery algorithms. ✓ denotes “support” whereas ✗ denotes “not support”.

Alg.	Orientation	FD-induced Faithfulness Violation	Causal Insufficiency
PC [46]	✓	✗	✗
FCI [52]	✓	✗	✓
REAL [14]	✗	✓	✗
XLEARNER	✓	✓	✓

Consequently, two challenges imposed by FD and causal insufficiency render popular causal discovery algorithms unsuitable for XDA. As reviewed in Table 2, there are currently solutions that handle the two challenges independently. REAL [14] studies causal discovery from causally sufficient data in the presence of FD-induced faithfulness violations, whereas FCI [52] aims to provide causal graphs from causally insufficient data under faithfulness assumptions. XLEARNER, for the first time, establishes a novel theory framework to synergistically combine and generalize existing solutions in order to *simultaneously address both issues*. Recall that FD causes faithfulness violations. XLEARNER provides a formal framework to identify the structures related to FDs prior to standard causal discovery. Once, FD-related structures are identified, sanitized variables (i.e., without faithfulness violations; see details in Sec. 3.1.1) are fed to the standard causal discovery algorithm. In this regard, XLEARNER conducts skeleton learning (identifying the undirected version of the causal graph) among FD-related nodes

and then perform orientation of FD-related edges. We outline the workflow of XLEARNER in Alg. 1 and then explain each module.

Algorithm 1: XLEARNER procedure.

```

Input: Database  $D$ , FD-induced graph  $G_{FD}$ 
Output: FD-augmented PAG  $G$ 
1 // phase 1: skeleton learning (Sec. 3.1.1)
2  $S \leftarrow (V, \emptyset)$ ;
3 Topologically sorting nodes in  $G_{FD}$  and record depth as  $d(X_i)$ ;
4 while  $G_{FD}$  has non-root nodes do
5    $X \leftarrow \operatorname{argmax}_{X \in G_{FD}, V} d(X)$ ;
6    $Y \leftarrow \operatorname{argmin}_{Y \in Pa(G_{FD}, X)} |Y|$ ;
7   add edge  $(X, Y)$  in  $S$ ;
8   remove  $X$  and all connected edges from  $G_{FD}$ ;
9 end
10  $S \leftarrow S \cup SL(D, G_{FD}, V)$ ;
11 // phase 2: orientation (Sec. 3.1.2)
12  $G \leftarrow FCI(S)$ ;
13 foreach  $(X \xrightarrow{FD} Y) \in G_{FD}.E$  do
14   | if  $X, Y$  is adjacent in  $G$  then orient  $X \rightarrow Y$  on  $G$  ;
15 end
16 return  $G$ ;

```

3.1.1 Skeleton Learning with FD. As pointed out in [14], under the presence of FD-induced faithfulness violations, we can at most obtain a *harmonious skeleton*. However, the original definition of *harmonious skeleton* is established under causal sufficiency. Here, we generalize the *harmonious skeleton* for causally insufficient systems:

DEFINITION 3.1 (HARMONIOUS SKELETON). A skeleton S is said to be *harmonious* w.r.t. a joint probability distribution P if 1) there exists a MAG G on the top of S , 2) P satisfies GMP to G , and 3) any subgraph of S does not satisfy the previous two conditions.

Def. 3.1 implies three key properties of the skeleton S . First, since there exists a MAG G on top of the skeleton S , there exists a set of nodes that m-separates any two non-adjacent nodes. Second, if a pair of nodes (such as X, Y) are m-separated, there exists a set of nodes (Z) such that $X \perp\!\!\!\perp Y | Z$. These two conditions imply that if X and Y are not connected in the skeleton S , then there must exist a set of nodes Z in the data such that $X \perp\!\!\!\perp Y | Z$. The last condition implies the minimality of skeleton, which is commonly assumed and in accordance with Occam’s Razor and human intuitions. When two MAG G, G' belong to the same Markov equivalence class, we usually prefer the simpler one. Therefore, if a skeleton S is harmonious, no subgraph skeleton S' satisfies the joint distribution. We now extend the main theorems from [14] for MAG, which begins with a basic case and generalizes to arbitrary structures.

THEOREM 3.1. If G_{FD} is single-sink graph whose sink is Z , a harmonious skeleton is $S = S_1 \cup S_2$, where S_1 is a harmonious skeleton over $\{X | X \in V \setminus \{Z\}\}$ learnt by any sound and complete skeleton learning algorithm, and S_2 contains $X_i - Z$ such that X_i can be any node in $V \setminus \{Z\}$.

We demonstrate an example of Theorem. 3.1 in Fig. 4. According to Theorem. 3.1, multiple harmonious skeletons exist for a multi-root single-sink FD-induced graph. Precisely, there are several possible S_2 , and Z can connect to either X_1, \dots, X_n . In practice, we choose the parent node with the lowest cardinality. Then, given an arbitrary FD-induced graph, we apply Theorem. 3.1 iteratively to form a harmonious skeleton (line 1–10 of Alg. 1).

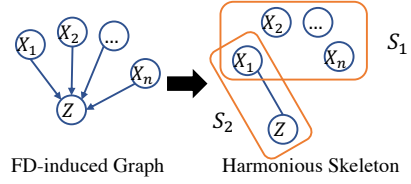


Figure 4: Example of single-sink G_{FD} .

THEOREM 3.2. The skeleton of Alg. 1 (line 1–10) is harmonious.

Alg. 1 first constructs an empty skeleton S that shares the same nodes as G_{FD} (line 2). At line 3, we topologically sort the G_{FD} nodes (note that G_{FD} is by definition a DAG). In each iteration (lines 5–8), we pick the deepest node and apply Theorem. 3.1 to connect X to one of its parents (in G_{FD}) Y in the skeleton. In our implementation, we use the parent node with the lowest cardinality as Y (line 6), as it usually aligns human intuitions. For root nodes, since there are no FDs and thus the faithfulness assumption holds, we employ the standard skeleton learning algorithm (line 10; SL can be any skeleton learning algorithms) to infer a harmonious skeleton over these variables. Finally, skeletons are concatenated to form a complete skeleton. By Theorem. 3.2, the final skeleton is harmonious.

3.1.2 Orientation. Classical constraint-based causal discovery algorithms decide the direction of edges based on a set of orientation rules. These rules orient undirected edges on skeletons (i.e., $\circ\circ$) based on a set of criteria, including conditional independence and some graphical structural relations (e.g., discriminating path) [52]. These rules are applied iteratively until no more orientation can be made. However, we argue that FD itself reflects practical causal relations to a good extent, whose reasons are twofold.

ANM Perspective on FD-related Edges. We anticipate to incorporate discrete additive noise model (ANM) [37] for orienting FD-related edges. The main theory of ANM implies that if an asymmetric ANM $Y = f(X) + N_Y$ exists from X to Y and N_Y is independent of X , then X causes Y . By FD, we note that, if $X \xrightarrow{FD} Y$ in G_{FD} , an ANM construction from Y to X exists only in very rare (impossible in practice) cases, as determined by the identifiability of discrete ANM (see Theorem. 4.6 in [38]). In light of this, we hypothesize that $X \xrightarrow{FD} Y$ in G_{FD} implies causation.

FCI Perspective on FD-related Edges. The rules in FCI may be unreliable due to the faithfulness violations by FDs. However, FD itself is generally more reliable, which precisely describes a form of deterministic relations. More importantly, the directions from FD are compatible with the result of FCI on the variables excluding FD-related variables. That is, the directions on FD-related edges is either be identical to FD’s direction or simply unidentifiable (i.e., $\circ\circ$). Therefore, incorporating ANM would not violate GMP.

We implement the above hypothesis as a post-processing step in our orientation algorithm (line 11–15 in Alg. 1). Initially, we apply FCI to orient the input skeleton as best it can (line 12). Then, we examine, for each FD relation that is also adjacent in G , the edge is oriented as \rightarrow (line 13–15). We note that, by incorporating ANM, the augmented graph is more informative and represents an over-complete graph w.r.t. the ground-truth MAG’s Markov equivalence class, exhibiting greater precision than causal graphs learned only by rules. We validate this in Sec. 4.3.

3.2 XTRANSLATOR

A causal graph does not directly reveal if a variable adequately explains a WHY QUERY, nor does it directly reflect if the variable features causal or non-causal explanation. Bridging this gap requires a translation from causal primitives to XDA semantics. To illustrate, we start with WHY QUERY under AVG through the lens of probability distribution. We then show how to generalize the main result into SUM and other aggregates.

Principle of Explainability. Given a WHY QUERY Δ where $agg = AVG$, a variable X is said to have *No Explainability* if $X \perp\!\!\!\perp M | F \cup B$, where M is the target measure, F is foreground variable, and B are background variable(s). In the subsequent discussion, we omit B for the ease of presentation without loss of generality.

A WHY QUERY in XDA requires us to observe the difference between aggregates on M within two subspaces. The conditional independence of $X \perp\!\!\!\perp M | F$ implies that $\mathbb{E}(M | F, X) = \mathbb{E}(M | F)$. Hence, $\Delta(D) \approx \Delta(D_{X=x})$ for all feasible filters in X . If X is *conditionally independent* of M , X is simply impossible to offer explanations to the WHY QUERY. Thus, this principle imposes a restriction on possible variables that have potentials to provide explanations. In particular, we derive the following restriction.

PROPOSITION 3.1. *If X has explainability, M, X are not m-separated by F in the causal graph G .*

Proposition 3.1 illustrates the chance of pruning variables that are impossible to provide explanations.

Table 3 depicts the translation from causal primitives to XDA semantics. In XTRANSLATOR, a variable X is first confirmed to have explainability if X, M are not m-separated by F in G (1st row in Table 3). In addition, XTRANSLATOR also categorizes whether X is causal or non-causal according to Table 3. Overall, X provides causal explanation if it is explainable and a cause (2nd and 3rd row in Table 3) or a possible cause (4th and 5th row Table 3) of M . This is intuitive, as an explanation should serve as a causal factor for the target, but not necessarily as the direct cause. For example, “Smoking” can be used to explain “Lung Cancer” (direct cause), and “Stress Level” can also be used to explain “Lung Cancer” (indirect cause). All other cases are conservatively treated as giving non-causal explanations (last row in Table 3). It is possible to derive a finer-grained explanation semantics within the non-causal explanation category, such as differentiating the cases where $M \rightarrow X$ or $M \leftrightarrow X$. We leave this as a future work.

Table 3: Translation between causal primitives and XDA semantics.

Path	Causal Primitive	XDA Semantics
$X \rightarrow F \rightarrow M, \dots$	m-separated	no explanability
$X \rightarrow M$	parent	causal explanation
$X \rightarrow \dots \rightarrow M$	ancestor	causal explanation
$X \circ \rightarrow M$	almost parent	causal explanation
$X \circ \rightarrow \dots \circ \rightarrow M$	almost ancestor	causal explanation
others	N/A	non-causal explanation

Extension to SUM. The above formulation over *explanability* is established on AVG aggregates. In the following, we discuss the implications of our formulation on SUM aggregates. If X has no explanability, $X \perp\!\!\!\perp M | F$. When we enforce $X = x$, $\Delta(D_{X=x})$ can merely be affected by the number of rows where $X = x$ in two sibling subspaces (namely a COUNT-based explanation) instead of

a causal relation between X and M (see detailed formulation in Supplementary Material [26]). This may be valid for explanations; nevertheless, it is typically inconsistent with the conventions of data analysis and may potentially violate user expectations regarding explanations (i.e., a variable explains the target). Furthermore, such COUNT-based explanations are non-conventional and is thus less concerned. In contrast, XTRANSLATOR focuses on the variables with strong connections to M , which are more likely to provide desirable explanations. Therefore, we believe that our concept of explainability serves a reasonable method for pruning uninformative variables for general aggregates, and we leave designing more comprehensive pruning rules for future exploration.

3.3 XPLAINER

XTRANSLATOR provides a coarse-grained, variable-level qualitative explanation to a WHY QUERY. For instance, “Smoking” is a causal explanation to “Lung Cancer” severity difference in Locations A and B. Furthermore, XPLAINER is designed to provide fine-grained predicate-level quantitative explanations (e.g., “Smoking=Yes” explains the difference with responsibility of 0.77 in Fig. 1(f)). XPLAINER is on the basis of a well-established framework, DB causality [28] (an extension of actual causality). Below, we rewrite the formulation of DB causality under the context of WHY QUERY.

DEFINITION 3.2 (DB CAUSALITY [28]). *Given a multi-dimensional data D and WHY QUERY Δ , let t be a tuple in D . t is called a counterfactual cause to Δ , if $\Delta(D) > \epsilon$ and $\Delta(D - \{t\}) \leq \epsilon$, where ϵ is a threshold defined by users. t is called an actual cause to Δ , if there exists a contingency $\Gamma \subseteq D$ such that t is a counterfactual cause for $D - \Gamma$ (i.e., $\Delta(D - \Gamma - \{t\}) \leq \epsilon < \Delta(D - \Gamma)$).*

DEFINITION 3.3 (DB RESPONSIBILITY [28]). *Suppose P is an actual cause to WHY QUERY Δ and Γ ranges over all valid contingencies for P . The responsibility of P is defined as $\rho_P = \frac{1}{1 + \min_{\Gamma} |\Gamma|}$, where $|\Gamma|$ denotes the number of tuples in the contingency.*

DB causality is appealing as it offers both a normalized measure ($\text{responsibility} \in (0, 1]$) and a contingency. First, when the responsibility is close to 1, it implies that the tuple is more accountable for the outcome, and when it hits 1, it is totally responsible. Second, the minimal contingency reflects the additional influential factors that, together with the tuple, are fully responsible to the outcome. The two elements form a quantitative explanation and are useful for users to understand why the difference exists.

3.3.1 Adaptation. However, DB causality is originally designed for data provenance. As pointed out in [31], tuple-level explanations are usually too fine-grained for data analysis scenarios. An individual tuple usually has too little effects on the highly aggregated outcome of a large dataset. Recalling the example in Fig. 1, users would expect to know that “Smoking=Yes” causes high “Lung Cancer” severity rather than an individual patient who is the cause of the high “Lung Cancer” severity. This necessitates predicate-level explanations which is more understandable and frequently used in data analysis scenarios and by many data explanation tools [3, 49]. Motivated by this, we make three adaptions over DB causality (namely, W-CAUSALITY, W-RESPONSIBILITY and conciseness) to support XDA. We formulate W-CAUSALITY as follows.

DEFINITION 3.4 (W-CAUSALITY). Given a multi-dimensional data D , an attribute of interest X and WHY QUERY Δ , let $P \subseteq \bigcup p_i$ be a predicate in D , where $\bigcup p_i$ denotes the set of all possible filters on X . P is called a counterfactual cause to Δ , if $\Delta(D) > \epsilon$ and $\Delta(D - D_P) \leq \epsilon$, where ϵ is a threshold defined by users. P is called a actual cause to Δ , if there exists a contingency $\Gamma \subseteq \bigcup p_i$ such that P is a counterfactual cause for $D - D_\Gamma$ (i.e., $\Delta(D - D_\Gamma - D_P) \leq \epsilon < \Delta(D - D_\Gamma)$), where $P \cap \Gamma = \emptyset$.

From Tuples to Predicates. In words, Def. 3.4 transforms tuple and contingency into two predicates. This way, explanation as well as contingency constitute a form of interventions over the multi-dimensional data. When a contingency Γ is applied, it indicates that, if the events related to Γ does not happen, then the events related to P is fully responsible for Δ . This adaptation in turn entails another adaptation to responsibility for predicate-level explanations.

DEFINITION 3.5 (W-RESPONSIBILITY). Suppose P is an actual cause to WHY QUERY Δ and Γ ranges over all validate contingencies for P . The responsibility of P is defined as $\rho_P = \frac{1}{1 + \min_{\Gamma} |\Gamma|_W}$, where $|\Gamma|_W$ is defined as $\max(\frac{\Delta(D - D_P) - \Delta(D - D_P - D_\Gamma)}{\Delta(D)}, 0)$. To ensure ρ_P is well-defined for all P , we let $\rho_P = 0$ if P is not a (counterfactual or actual) cause and $\rho_P = 1$ if P is a counterfactual cause.

W-RESPONSIBILITY. Instead of using the number of rows in D_Γ as $|\Gamma|_W$, Def. 3.5 employs the truncated difference of Γ over Δ to measure the importance of P . In particular, $\Delta(D - D_P) - \Delta(D - D_P - D_\Gamma)$ can be deemed as *first-order finite backward difference* to the function $\Delta(\cdot)$ at the point of $D - D_P$ and Γ is the step size. This supplies a simple and intuitive way to understand to what extent Γ plays an important role in reducing the difference. Large difference imposed by Γ implies low importance of explanation P to Δ ; because the reduction on Δ is primarily caused by Γ instead of P itself. Therefore, the responsibility of P is measured by a validate contingency Γ^* (such that $\Delta(D - D_P - D_\Gamma) \leq \epsilon$ and $\Delta(D - D_\Gamma) > \epsilon$) with minimal difference on Δ .

Conciseness. Using responsibility as the sole criterion is not sufficient in practical data analysis scenarios [17]. Typically, a *concise* explanation is preferable. Therefore, given an attribute of interest X , we formulate the optimal explanation of X as follows.

$$\operatorname{argmax}_{P \subseteq \bigcup p_i} \rho_P - \sigma|P| \quad (3)$$

where $\bigcup p_i$ is the set of all possible filters in X , $|P|$ is the number of filters in P , and $\sigma|P|$ ($\sigma > 0$) forms a conciseness regularization.

3.3.2 Optimization. As pointed out in [8, 9], computing responsibility (i.e., ρ_P) is intractable. Furthermore, solving the optimization problem in Eqn. 3 is itself difficult given 2^m search space (m is the number of filters in X). In the following paragraphs, we design specific optimizations for SUM and AVG. In short, we show that a linearithmic approximated solution exists for the problem when the aggregation is SUM, and we provide a heuristics-based solution for AVG with quadratic complexity. Our empirical results (Sec. 4.4) show that the approximation is tight and efficient.

Optimization for SUM. Given the additive property of SUM (i.e., $\Delta(D_{P_1} + D_{P_2}) = \Delta(D_{P_1}) + \Delta(D_{P_2})$), we obtain the following proposition to prune the search space.

PROPOSITION 3.2. If P^* is the optimal explanation of Eqn. 3, $\forall p \in P^*, \Delta(D_p) > 0$.

According to Proposition. 3.2, the search algorithm can omit filters with non-positive Δ_i (i.e., $\Delta(D_{p_i})$). Recall that Eqn. 3 seeks the optimal explanation. When the aggregate function is SUM, we only need to focus on filters with reasonably high Δ_i without losing optimality and we define such filters as *canonical filters*.

DEFINITION 3.6 (CANONICAL FILTER AND PREDICATE). Without loss of generality (w.l.o.g.), given a WHY QUERY Δ and an attribute of interest X , let filters $\{p_1, \dots, p_m\}$ of X is ordered by Δ_i (i.e., $\Delta(D_{p_i})$) such that $\Delta_1 \geq \dots \geq \Delta_m$. We let p_1, \dots, p_j be canonical filters if

$$\Delta(D) - \sum_{i=1}^j \Delta_i \leq \epsilon < \Delta(D) - \sum_{i=1}^{j-1} \Delta_i \quad (4)$$

Accordingly, $P^C = \{p_1, \dots, p_j\}$ is called canonical predicate and we let $\tau = \sum_{i=1}^j \Delta_i$.

With canonical filters and corresponding canonical predicate P^C , we observe that P^C manifests nice properties. First, P^C is the minimal counterfactual cause entailed by Eqn. 4. Our construction of canonical predicates guarantees completeness.

PROPOSITION 3.3 (COMPLETENESS). For SUM, given a WHY QUERY Δ , an attribute of interest X and corresponding canonical predicate P^C , there exists an optimal explanation $P^* \subseteq P^C$.

The completeness proposition (Proposition. 3.3) allows us to only focus on canonical filters when searching the optimal explanation without the loss of optimality. More importantly, canonical predicate also allows us efficiently identify actual causes and the corresponding valid contingencies.

THEOREM 3.3. For SUM, given a WHY QUERY Δ , an attribute of interest X and corresponding canonical predicate P^C , $\forall P \subset P^C$, P is an actual cause and $\bar{P} = P^C - P$ (the complement set of P) is a valid contingency.

The advantage of Theorem. 3.3 is twofold. First, we can directly confirm valid explanations without exhaustive enumerations. Second, by the property of \bar{P} , we bound P 's responsibility (ρ_P).

THEOREM 3.4. For SUM, given a WHY QUERY Δ , an attribute of interest X and corresponding canonical predicate P^C , the W-RESPONSIBILITY ρ_P of $P \subset P^C$ satisfies

$$\frac{1}{1 + \frac{\tau - \Delta(D_P)}{\Delta(D)}} \leq \rho_P \leq \frac{1}{2 - \frac{\Delta(D_P) + \epsilon}{\Delta(D)}} \quad (5)$$

When $\Delta(D_P) \ll \tau$ and $0 < \tau \leq \Delta(D)$, $\frac{1}{1 + \tau - \Delta(D_P)} \approx \frac{1 + \tau + \Delta(D_P)}{(1 + \tau)^2}$ and the corresponding approximation error rate $E < 0.25$.

Theorem. 3.4 provides a way to efficiently approximate responsibility with theoretical guarantees. In that sense, we can compute responsibility immediately and alleviate searching the minimal contingency. Let $\hat{\rho}_P = \frac{1 + \tau + \Delta(D_P)}{(1 + \tau)^2}$, we can rewrite the objective function in the following form.

$$\hat{\rho}_P - \sigma|P| = C_1 + C_2 \times \sum_{p_i \in P} (\Delta_i - C_3) \quad (6)$$

Here, C_1, C_2, C_3 are constants. Then, the optimal explanation to Eqn. 6 is straightforward:

$$P^* = \{p_i \mid \Delta_i > C_3\} \quad (7)$$

where $C_3 = \frac{\sigma\Delta(D)}{(1 + \frac{\epsilon}{\Delta(D)})^2}$. The complexity is $O(m \log(m))$ (primarily in sorting filters for generating canonical predicates).

Optimization for AVG. In terms of AVG, it is generally much more challenging due to the absence of the additive characteristics on $\Delta(D_p)$. Therefore, the majority of the preceding propositions are not applicable. Having that said, we find the causal graph gives considerable opportunities to prune unnecessary computations.

DEFINITION 3.7 (HOMOGENEOUS SIBLING SUBSPACE). *Given sibling subspaces s_1, s_2 (with foreground variable F and background variables B), an attribute X and the causal graph G , s_1, s_2 are homogeneous on X if X, F are m -separated given B on G .*

PROPOSITION 3.4. *For homogeneous AVG, given a WHY QUERY Δ , an attribute of interest X , a predicate $P \subseteq \bigcup p_i$ and a filter $p \in P$, if $\Delta(D_p) > \Delta(D_p)$, then $\Delta(D_p - D_p) < \Delta(D_p)$.*

To practically address the search problem of AVG (Eqn. 3), we rely on a greedy-based heuristics with pruning strategy enabled by Proposition. 3.4. The algorithm is outlined in Alg. 2.

Algorithm 2: XPLAINER For AVG

```

Input: WHY QUERY  $\Delta$ , threshold  $\epsilon$ , consisness parameter  $\sigma$ 
Output: (near) optimal explanation  $P^*$ 
1  $P^C \leftarrow \emptyset$ ;
2 foreach  $r = 1, \dots, \min(m, \frac{1}{\sigma})$  do;
3   if  $\Delta(D - D_{P^C}) \leq \epsilon$  then break;
4   else
5      $\bar{P} \leftarrow \{p_1, \dots, p_m\} - P^C$ ;
6     if homogeneous then
7        $S \leftarrow \{p_i \mid p_i \in \bar{P}, \Delta_i > \Delta(D - D_{P^C})\}$ ;
8        $p^* \leftarrow \operatorname{argmin}_{p \in S} \Delta(D - D_{P^C} - D_p)$ ;
9     else
10       $p^* \leftarrow \operatorname{argmin}_{p \in \bar{P}} \Delta(D - D_{P^C} - D_p)$ ;
11    end
12     $P^C \leftarrow P^C \cup \{p^*\}$ ;
13  end
14 end
15 if  $\Delta(D - D_{P^C}) > \epsilon$  then return  $\perp$ ;
16 foreach  $k \in 1, \dots, |P^C|$  do
17    $P_k \leftarrow$  top-k filters of  $P^C$ ;
18    $\Gamma_k \leftarrow P^C - P_k$ ;
19   compute  $\rho \hat{P}_k$  with  $\Gamma_k$ .
20 end
21 return  $\operatorname{argmax}_k \rho \hat{P}_k - \sigma |P_k|$ ;

```

The high-level idea behind Alg. 2 is similar to the one for SUM, which attempts to construct a canonical predicate P^C such that P^C forms a counterfactual cause, each subset $P \subset P^C$ of the canonical predicate constitutes an actual cause, and the complement set $P^C - P$ is a valid contingency. Unlike SUM, however, Alg. 2 does not ensure the optimality of the resulting explanation, primarily due to the incompleteness of canonical predicate (Proposition. 3.3) under AVG. Recall Eqn. 3, where ρ_P ranges from 0 to 1. The optimal explanation contains at most $1/\sigma$ filters (otherwise, $\rho_P - \sigma |P| < 0$). Hence, the canonical predicate P^C shall contain at most $1/\sigma$ or m (i.e., the number of filters in the attribute).

Alg. 2 employs a greedy strategy to construct P^C progressively. It starts with an empty canonical predicate (line 1) and insert one

filter in each iteration (lines 2–13). Before insertion, it first checks whether P^C is a canonical predicate (line 3) and terminates the loop if P^C is already valid. Otherwise, it picks the remaining filters that were not chosen in earlier iterations as candidates (line 5) and inserts the filter that minimizes the difference $\Delta(D - D_{P^C} - D_{p_i})$ at the highest magnitude into P^C (lines 6–12). When homogeneity holds and $\Delta_i \leq \Delta(D - D_{P^C})$, Alg. 2 prunes p_i according to Proposition. 3.4 (lines 7–8). Note that Δ_i is invariant throughout the loop; thus it only needs to be queried once. In general cases where homogeneity does not hold, Alg. 2 has to enumerate all possible filters in \bar{P} (line 10). If we cannot obtain a valid canonical predicate (i.e., a counterfactual cause to Δ) after the loop, Alg. 2 terminates and outputs \perp , indicating that it fails to find the optimal explanation within the attribute (line 15). Empirically, we does not observe such rare cases. When the canonical predicate P^C is obtained, $\forall k = 1, \dots, |P^C| - 1$, the top-k filters of $P_k \subseteq P^C$ is a valid actual cause and the complement set $\Gamma_k = P^C - P_k$ is a valid contingency. According to the termination condition in the above loop (line 3), $\Delta(D - D_{P_k}) > \epsilon$. And according to the definition of canonical predicate $\Delta(D - D_{P^C}) = \Delta(D - D_{P_k} - D_{\Gamma_k}) \leq \epsilon$, Γ_k is a valid contingency to P_k . Therefore, we compute the approximated responsibility $\rho \hat{P}_k$ by using its lower bound deduced by Γ_k (line 19). After enumerating each k , Alg. 2 returns P_k such that $\rho \hat{P}_k - \sigma |P_k|$ is maximized (line 21). In summary, the first loop (lines 2–14) is of quadratic complexity regardless of homogeneity and the second loop is linear (lines 16–20). The total complexity is $O(m^2)$.

4 EVALUATION

In this section, we evaluate XINSIGHT to answer the following three research questions (RQs):

- (1) **RQ1: End-To-End Performance.** How could XINSIGHT facilitate end users in explainable data analysis?
- (2) **RQ2: XLEARNER Evaluation.** Does XLEARNER effectively recover causal relations from observational data?
- (3) **RQ3: XPLAINER Evaluation.** Does XPLAINER accurately and efficiently yield explanations?³

4.1 Datasets

To the best of our knowledge, there is no real-world benchmarks with manually labeled query/explanation pairs. To deliver a scientific evaluation, we conduct experiments on ① public datasets collected from previous works, ② real-world data collected from production environment for user study and human evaluation, and ③ synthetic data with ground-truth explanations. The detailed steps for constructing synthetic datasets are given in Supplementary Material [26]. We make necessary preprocessing before feeding to XINSIGHT (e.g., remove missing value).

① **Flight Delay (FLIGHT).** We use the flight delay dataset from [43] to explore the causes of flight delays in US airports. After preprocessing, the resulting dataset contains 17 variables, including the weather conditions of departure airports (temperature, humidity, visibility, rain, etc.), flight carrier, flight time (month, quarter, year, day of week and hour) and two variables indicating flight delays, DelayMinute (continuous) and Delay>15min (binary).

³The correctness of XTRANSLATOR has been rigorously proved in Sec. 3.2.

① **Hotel Booking (HOTEL).** The hotel booking dataset [6] is frequently used for demonstrating data analysis methods. It contains 119,390 observations from two hotels. Each observation depicts the booking status (e.g., “room type”, “reservation status”, and “is canceled”) of a guest in a hotel.

Table 4: Web Service Behavior Dataset.

ClickButton1	ClickButton2	CopyLink	DownloadFile	...	IsBlocked
Yes	No	Yes	No	...	Yes
...

② **Web Service Behavior Dataset (WEB).** The dataset is collected from a web service’s production environment. It contains 29 columns and 764 rows, where each row is a list of binary values. As depicted in Table 4, the first 28 columns describe a user’ behaviors on the web service (e.g., whether he clicks a specific button), which are collected by a logging module. The last column indicates whether the user has been blocked for publishing malicious content (i.e., “IsBlocked”), which is annotated by cybersecurity experts. These behaviors are known to exhibit strong and clear causal relations, making them appropriate for testing XINSIGHT in real-world scenarios. We use this dataset to deliver an end-to-end evaluation and to assess XLEARNER based on the identified causal relations.

③ **Synthetic Data A (SYN-A).** Ground-truth causal graphs are unattainable in practice and it is common to generate random graphs and then sample observational data from this graphical model. We generate MAGs with 10 to 150 variables (141 distinct scales in total). For each scale, we synthesize five random graphs and the associated datasets, resulting in 705 (141 \times 5) datasets.

③ **Synthetic Data B (SYN-B).** We follow the approach in Scorpion [49] to synthesize datasets for assessing XPLAINER. Each dataset includes a valid WHY QUERY and a ground-truth explanation to this difference. We generate 18 datasets of different difficulties.

4.2 RQ1: End-To-End Performance

We show that XINSIGHT generates plausible and intuitive explanations for diverse datasets (**FLIGHT**, **HOTEL** and **WEB**) and invite experts to assess the quality of explanations generated for **WEB**. In this experiment, we manually discover noticeable differences to form WHY QUERY, and ask XINSIGHT to supply the explanations. We also compare XINSIGHT’s outputs with naive correlation-based explanations. To ease presentation, we describe WHY QUERY in human-readable natural language in the following paragraphs.

FLIGHT & HOTEL. We ask the following WHY QUERY on ①:

- (1) FLIGHT: *why AVG(DelayMinute) in May (24.95 min) is notably higher than the one in November (21.28 min)?*
- (2) HOTEL: *why AVG(IsCancelled) (cancellation rate) in July (0.37) is notably higher than the one in January (0.30)?*

For the first WHY QUERY, we observe that the duration of flight delay differs in month, particularly for May and November, which motivates us to ask XINSIGHT for explanations – what is the cause of the flight delay difference. XINSIGHT first learns a causal graph from data which identifies “rain” as a direct cause to DelayMinute. Then, XPLAINER finds that the difference is reversed ($\Delta = 3.674$ vs. $\Delta' = -2.068$) when the condition “rain=Yes” is enforced. Thus, it returns “rain=Yes” as an explanation, as shown in Fig. ???. We interpret the explanation as correct because 1) rain is a typical reason for flight

delay, and 2) for many states in US, monthly precipitation in May is usually higher than the one in November. Therefore, when only counting the rainy cases (by enforcing “rain=Yes”), the difference is eliminated and even reversed, given that rain in November usually associates snow which further affects flight time.

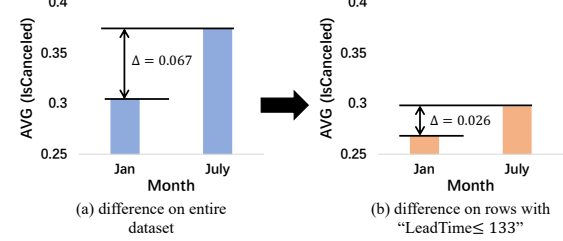


Figure 5: Explanation to WHY QUERY on the HOTEL dataset.

For the second WHY QUERY, we observe that the cancellation rate varies by month of arrival. For instance, the cancellation rate in July is 0.37, which is higher than the one in January. Thus, we ask XINSIGHT for explanations. XINSIGHT identifies “LeadTime” (number of days between booking data and arrival date) as an indirect cause of “IsCancelled”. It also discovers, as depicted in Fig. 5, that when enforcing “LeadTime ≤ 133 ”, the difference is reduced. This is intuitive. Longer “LeadTime” results in greater uncertainty on guests’ future schedules, leading to a higher cancellation rate. In January, LeadTime of most reservations is less than 133 days (91%). In contrast, there are much more early reservations (> 133 days) in July (48%), resulting in a higher cancellation rate. When these early reservations are excluded, the difference becomes much smaller.

WEB. In this dataset, we primarily focus on the difference in the “IsBlocked” column, as the difference and accompanying explanations are useful for experts constructing detection methods for malicious behaviors. We ask a total of four WHY QUERY and for each WHY QUERY, we use XINSIGHT to generate explanations of every causal variable and we pick the ranked top-2 causal variables/explanations with the highest responsibility score. Given a total of eight WHY QUERY-explanation pairs, we ask human experts to rate each pair a score (between 0 to 5) based on their domain knowledge of **WEB** and to provide their overall opinion of XINSIGHT.

Table 5: Human assessment on explanations generated by XINSIGHT. E_i stands for the i th explanation and P_i stands for the i th human participant.

	E1	E2	E3	E4	E5	E6	E7	E8
P1	4	4	5	4	4	4	5	3
P2	4	4	4	4	3	4	3	4
P3	5	3	4	5	3	5	5	5
P4	3	4	5	4	4	3	3	4
mean	4.00	3.75	4.50	4.25	3.50	4.00	4.00	4.00
std	0.71	0.43	0.50	0.43	0.50	0.71	1.00	0.71

Human assessment results are in Table 5. We view the results as encouraging as all feedbacks are positive (≥ 3). Moreover, the average score for six out of eight explanations is at least 4.0. After the assessment on each explanation, experts find many explanations are inspiring and insightful, despite their familiarity with the dataset (note that these participants are developers or product managers of this web service). It increases their knowledge and enables them to design better criteria for detecting malicious behavior.

Answer to RQ1

XINSIGHT manifests promising end-to-end performance in data difference explanation. Human assessment experiments show that *XINSIGHT* achieves a respectable level of agreement with human experts.

4.3 RQ2: XLEARNER Effectiveness

As a cornerstone of XINSIGHT, XLEARNER is crucial to the effectiveness of the entire pipeline. To answer **RQ2**, we use a set of approaches commonly taken in the causality community to conduct direct and indirect evaluations of XLEARNER.

4.3.1 Evaluation on Synthetic Dataset. We report the F1 Score, precision and recall of the output with respect to the PAG ground-truth. In accordance with prior works, we consider *partial match* which treats \circ as a wildcard edge endpoint (see Table 1). Either an arrow or a tail on the endpoint would be considered matched, because the joint probability distributions are Markov indistinguishable.

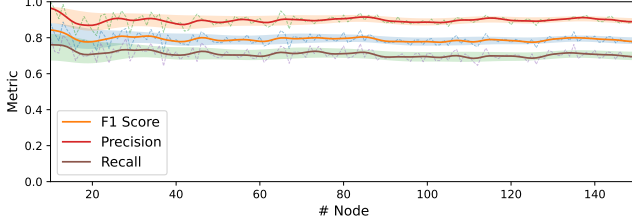


Figure 6: XLEARNER on synthetic data.

Fig. 6 reports the result of running XLEARNER on the 705 datasets in **SYN-A**. We interpret the result as promising, where the vast majority of edges are correctly identified by XLEARNER. As in Fig. 6, XLEARNER manifests consistently encouraging accuracy on datasets with varied scales, with performance not degrading considerably as datasets are scaled. We also compare XLEARNER and FCI algorithms in Table 6. Note that FCI can be seen as an ablated version of XLEARNER without special treatment on functional dependencies. Their performance is comparable, with XLEARNER being relatively superior. Given that functional dependencies typically constitute a small portion of the PAG (and hence the likelihood of FD-induced faithfulness violations is low), we interpret the comparison result as reasonable. Furthermore, the high precision and recall also indicate that XLEARNER (along with other causal discovery algorithms) is mature for recovering causal relations from observational data.

Table 6: Comparison between XLEARNER and FCI.

Algo.	F1-Score	Precision	Recall
XLEARNER	0.79 ± 0.06	0.90 ± 0.06	0.71 ± 0.07
FCI (XLEARNER w/o FD)	0.76 ± 0.07	0.89 ± 0.06	0.68 ± 0.07

4.3.2 Evaluation on Real-world Data. In addition to the experiments on synthetic datasets, we also evaluate XLEARNER with the **WEB** dataset (Sec. 4.1). As aforementioned, this real-world dataset lacks a ground-truth causal graph. Evaluating the accuracy of an estimated causal graph is thus challenging, if not impossible. At this step, we apply indirect assessment methodologies to compare XLEARNER with its competitors through the lens of **Causal Feature Selection**. Also, in addition to these quantitative experiments,

we conduct a **Human Evaluation** by involving human experts to assess the correctness of the identified causal relations.

Causal Feature Selection. Given a variable X in a causal graph with variable set V , there exists a useful property that its Markov boundary (i.e., minimal Markov blanket) $MB(X)$ renders X conditionally independent of all other variables. Formally, $X \perp\!\!\!\perp V \setminus X \cup MB(X) \mid MB(X)$, which implies that $MB(X)$ is the minimal feature subset with the highest predictability, as all other features are conditionally independent of the target variable conditioning on its MB [51]. In theory, $MB(X)$ supplies the optimal predictive power that we can obtain from the full feature collection V . And in practice, feature selection based on $MB(X)$ often achieves higher robustness against domain shifting. In most settings, X 's neighbors (i.e., its parents and children) suffice as its Markov boundary. Thus, we use the accuracy of causal feature selection to estimate whether XLEARNER outputs a plausible local structure of X .

Table 7: Predictability of suggested features. $Acc_{1,2,3}$ stands for the accuracy Logistic Regression, Support Vector Machine, and Decision Tree models, respectively. Acc_{avg} is the average.

Algo.	Acc ₁	Acc ₂	Acc ₃	Acc _{avg}
XLEARNER	0.918 ± 0.038	0.916 ± 0.042	0.923 ± 0.026	0.919
MI	0.897 ± 0.038	0.902 ± 0.042	0.904 ± 0.042	0.901
Apriori	0.777 ± 0.052	0.765 ± 0.046	0.820 ± 0.029	0.787
DIFF	0.863 ± 0.048	0.865 ± 0.047	0.885 ± 0.050	0.871
Scorpion	0.903 ± 0.042	0.902 ± 0.046	0.903 ± 0.039	0.903

We consider two families of baselines for comparison: 1) *Mutual Information* (*MI*) and *Apriori* (*Frequent Itemset Mining*) [4] that use the top-k relevant features of “IsBlocked” to train the regression model; 2) *DIFF* [3] and *Scorpion* [49] that use the columns associated to the top-k explanations on the difference between the count of “IsBlocked=Yes” and “IsBlocked=No”. To ensure a fair comparison, we allow all feature strategies to use the same feature size, where k is the number of parents and children of “IsBlocked” in the XLEARNER output. These baselines are considered non-causal methods for explaining queries on “IsBlocked”. Using the aforementioned feature selection strategies, we train logistic regression models, support vector regression models, and decision tree regression models, and report the mean error under 10-fold cross validation in Table 7. We observe that XLEARNER achieves the minimal average error across the three models. In contrast, models trained with baseline strategies are often suboptimal, indicating that stronger correlations reflected by these baselines do not necessitate strong causal relations that enhance predictability.

Human Evaluation. In addition to the quantitative evaluation launched above, we intend to determine the extent to which the identified causal relation is correct and reasonable to human experts. Thus, we conduct a human evaluation to assess the validity of the causal relations identified by XLEARNER. We invite four participants to this human evaluation session, who are engineers or product managers of the web service with sufficient knowledge of this dataset. Given that enumerating all edges would be overwhelming for participants, we only consider the edges associated with the *IsBlocked* node, which is the primary focus of the dataset. Recall that different edges relate to diverse causal semantics (as shown in Table 1). We organize the human evaluation as follows:

- (1) **Participant Education.** We organize an education session to participants and demonstrate how to discern between causation and correlation. Then, a pilot study is conducted to confirm that participants have an adequate sense of causality.
- (2) **Causal Claim Assessment.** Following [22], we transform causal relations into human-comprehensible natural language assertions and ask participants to independently evaluate them.
- (3) **Follow-up Discussion.** Participants explain their decision and discuss the aggregated results.

We consider the edges with unambiguous meanings (see Table 1) in the human evaluation. In particular, we collect eight edges connected to “IsBlocked”. The human evaluation consists eight questions, where seven of them are bidirectional (\leftrightarrow), and one is directional (\rightarrow). For bidirectional and directional edges that are of unambiguous meanings (see Table 1), we ask participants to label them as “reasonable,” “not reasonable,” or “unsure” (eight questions).

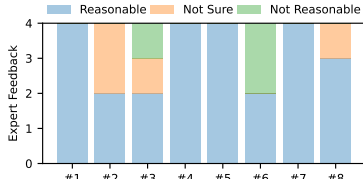


Figure 7: Expert feedbacks on causal claims.

We report our findings in Fig. 7: first, out of 32 (4 participants \times 8 question) feedbacks, only 3 feedbacks (9.4%) suggest that the causal claims are “not reasonable,” while 25 feedbacks (71.9%) mark the causal claims as “reasonable.” It indicates that the causal relations identified by XLEARNER correspond with expert knowledge in the majority of instances. Second, we investigate further the claims that have been deemed “not reasonable” or “unsure.” Surprisingly, we find that a notable proportion of causal claims are counter-intuitive yet *correct*. For instance, one causal claim states that “malicious intent would lead to more frequent configuration changes than benign intent.” In the causal claim assessment phase, one expert deemed it “not reasonable” and presumed that malicious users would keep default configuration. In the follow-up session where they shared the independent assessments, this participant was persuaded and confirmed this causal relation as “reasonable.”

Answer to RQ2

As reflected by a set of carefully-designed quantitative experiments and human evaluations, XLEARNER generates plausible causal graphs. Compared to existing baselines, causal graphs identified by XLEARNER are generally more accurate and useful for downstream tasks.

4.4 RQ3: Efficiency of XPLAINER

Recall the descriptions of **SYN-B** in which different parameters result in datasets with varying degrees of difficulty. In this experiment, we explore the accuracy (i.e., if the ground-truth explanation is among the top-3) of XPLAINER on **SYN-B** and compare it with Scorpion [49], a lightweight algorithm that finds the predicate with the highest influence. To setup Scorpion, we let $X = 1$ be the outlier

region and $X = 0$ be the hold-out results, and we compute the influence score using $\lambda = 0.75$.⁴ Given that Scorpion generates top-k expectations and XPLAINER generates one optimal explanation, we compute the F1 Score of filters in the optimal explanations given by XPLAINER and Scorpion against the ground-truth expectation.⁵ We now evaluate XPLAINER from different aspects.

Table 8: XPLAINER and Scorpion under various settings. ✓ denotes the result is identical to the ground truth (F1=1.0).

	# Rows (Cardinality=10)	10K	20K	50K	100K	500K	1M
XPLAINER (SUM)	F1 Score	✓	✓	✓	✓	✓	✓
	Time (sec.)	0.004	0.005	0.007	0.010	0.017	0.019
Scorpion (SUM)	F1 Score	0.5	0.5	0.5	0.5	0.5	0.8
	Time (sec.)	0.15	0.19	0.31	0.49	0.63	0.72
XPLAINER (AVG)	F1 Score	✓	✓	✓	✓	✓	✓
	Time (sec.)	0.016	0.019	0.026	0.038	0.052	0.063
Scorpion (AVG)	F1 Score	✓	✓	✓	✓	✓	✓
	Time (sec.)	0.12	0.14	0.19	0.28	0.38	0.43
Cardinality (# Rows=100k)	10	15	20	30	50	100	
XPLAINER (SUM)	F1 Score	✓	✓	✓	✓	✓	0.8
	Time (sec.)	0.010	0.014	0.018	0.025	0.040	0.077
Scorpion (SUM)	F1 Score	0.5	0.5	0.5	0.5	0.5	0.5
	Time (sec.)	0.49	1.71	4.12	13.92	66.41	536.20
XPLAINER (AVG)	F1 Score	✓	✓	✓	✓	✓	✓
	Time (sec.)	0.038	0.060	0.082	0.124	0.211	0.426
Scorpion (AVG)	F1 Score	✓	✓	✓	✓	✓	0.8
	Time (sec.)	0.28	0.96	2.28	7.71	35.88	288.74

Different Dataset Size. To study the scalability of XPLAINER, we generate datasets with different sizes and report the results in Table 8. Overall, we observe that XPLAINER has higher accuracy and efficiency compared to Scorpion. In particular, Scorpion often produces incomplete explanations, while the XPLAINER’s explanation are usually consistent with the ground truth. We presume that this is because Scorpion was built for explaining anomalies instead of WHY QUERY. Furthermore, XPLAINER is highly efficient regardless of the number of rows or the cardinality of attributes. We note that some optimizations mentioned in [49] may help improve Scorpion’s performance while sacrificing some accuracy. In sum, we interpret that XPLAINER delivers highly encouraging accuracy and efficiency.

Table 9: XPLAINER and Scorpion with different $\mu^* - \mu$. ✓ denotes the result is identical to the ground truth (F1=1.0).

$\mu - \mu^*$	5	10	15	30	50	100
XPLAINER (SUM)	0.86	✓	✓	✓	✓	✓
Scorpion (SUM)	0.50	0.50	0.50	0.50	0.50	0.50
XPLAINER (AVG)	✓	✓	✓	✓	✓	✓
Scorpion (AVG)	0.80	✓	✓	✓	✓	✓

Different $\mu^* - \mu$. The difference between μ^* , μ indicates the magnitude of Δ . To study the sensitivity of XPLAINER, we study how well does XPLAINER perform under subtle differences and compare it with Scorpion in Table 9. On SUM aggregates, we find that both Scorpion and XPLAINER have difficulties on identifying explanations when the difference is subtle (i.e., $\mu^* - \mu = 5$). Having that said, XPLAINER generally recovers more accurate explanations while Scorpion is often sub-optimal on SUM. This observation is consistent with the result in Table 8. On AVG aggregates, both XPLAINER and Scorpion are equally good and successfully identify the ground-truth explanations. We omit to report the processing time here, since it has been evidently explored in Table 8.

⁴Scorpion originally employs $\lambda = 0.5$ while we find $\lambda = 0.75$ yields more accurate expectations in all settings.

⁵We implement the NAIVE partitioner and BASIC merger of Scorpion described in their paper, where queries are conducted on the same DBMS of XPLAINER. Explanations are searched from $P \subset 2^Y$, $|P| \leq 3$ and 2^Y denotes the power set of filters in Y .

Tightness of Approximation. In Sec. 3.3, we show the approximation of minimal contingency for computing responsibilities under SUM and AVG. In the following, we compare the tightness on the responsibility $\hat{\rho}$ computed by $\bar{P} = P^C - P$ to the true responsibility ρ computed by the minimal contingency P_{\min} via brute-force search. The approximation error is computed as $E = \frac{|\hat{\rho} - \rho|}{\rho}$. Recall that we craft three filters that form the counterfactual cause in each dataset. On SUM, we can craft six ($\binom{3}{2}$) actual causes from the three filters. On AVG, since the canonical predicate of AVG only supports first k filters as actual causes and the rest as contingency, we pick the top-1 and top-2 filters as two actual causes and repeat the experiments on three datasets (2×3 in total). On the six actual causes of SUM aggregates, we find that the brute-force algorithm is $253.3 \times$ slower than our approximated solution. More importantly, the approximation error is highly negligible with an average of 0.007. We also observe that the approximation error on AVG is slightly higher than the one of SUM (0.066) and that our heuristics-based solution is $27.3 \times$ faster. We interpret this result as reasonable, as the heuristics-based solution does not provide guarantees on accuracy and requires more queries than SUM.

Answer to RQ3

XPLAINER shows high scalability to large datasets and also accurately generates explanations in very difficult settings. On a mild cost of precision, two approximation solutions of XPLAINER substantially improves efficiency.

5 DISCUSSION

Single Dimension Explanation. XINSIGHT primarily focuses on explanation over a single dimension. However, we observe many data explanation tools may returns explanations with multiple dimensions (e.g., “Stress=High” and “Smoking=Yes” explains high lung cancer severity). Technically, XINSIGHT can be smoothly extended to such cases by cartesian product on multiple dimensions. However, conceptually, such multiple dimensions may impose complicated (and even obscure) causal semantics. Hence, XINSIGHT only considers single dimension explanations.

Other Forms of Explanations. Currently, XINSIGHT employs predicates as the content of explanations, which is general enough for common data analysis scenarios. However, we clarify that, in some cases, explanations may be formed by the number of records in database [2] or counterbalances [32]. Furthermore, when explaining changes of whole time series [11], XINSIGHT may be not applicable. We leave integrating XINSIGHT into these scenarios for future work.

6 RELATED WORK

Data Explanation. Explaining an unexpected query outcome in database is a crucial phase in the lifecycle of data analysis. In general, an explanation aims to provide certain form of patterns such that lead to the unexpected query outcome. Such patterns may be a set of predicates [3, 7, 42, 49], tuples [31] or counterbalances [32]. Scorpion is the most relevant work to XINSIGHT, which also provides explanations to aggregated queries [49]. In particular, it employs an

influence score to quantify explanations and features a set of optimizations to reduce the cost of explanation search. Recently, many tools attempt to enhance explanations with additional knowledge (e.g., join table) about the underlying data. However, such additional knowledge does not imply causation – top ranked explanations could be rated low by human participants due to a lack of causal semantics [23]. The observation evidently shows the necessity of integrating causality into XDA.

Acquiring Causal Knowledge. Inferring causal relations is difficult. Typically, it needs a combination of domain knowledge [5], randomized experiments [47] and causal discovery [12, 14, 24, 46, 52]. XINSIGHT performs causal discovery from observational data due to its simplicity. Nevertheless, we envision users of XINSIGHT can combine additional sources for acquiring more accurate causal knowledge. In this paper, we consider the unique challenges of applying causal discovery to real-world data, namely causal insufficiency [52] and FD-induced faithfulness violations [14, 27]. XLEARNER, for the first time, simultaneously addresses them.

Causality in Database. Most works related to causality analysis in database is on the basis of Halpern’s seminal framework on actual causality [18, 19]. It provides a elegant and natural way to reason the relation between input and output; and its results not only highlight the cause of the output but also a contingency indicating how it is triggered. The adaptation of actual causality in database (i.e., DB causality) is widely used for data provenance [29], data explanation [42] and debugging [15, 30, 50]. Having that said, it has limitations when being applied alone. On one hand, as is pointed out in [17], DB causality does not implies *true causation*. Indeed, it takes causal knowledge as prior knowledge and merely deals with quantitative explanations. On the other hand, considerable adaptations are needed to make it suitable for XDA scenarios, as have been discussed in Sec. 3.3. We also notice other methods for quantifying explanations such as sufficient score, necessity score, average causal effect [44, 48]. Despite their usefulness, we design XPLAINER on the top of actual causality because it is more understandable and general. Furthermore, without causal knowledge as a prior, all these methods cannot implies true causation.

XDA vs. XAI. We note that XAI (explainable artificial intelligence) is parallel and complement to XDA. Through the lens of data analysis, XAI aims to provide explainability for predictive data analysis (e.g., explaining a prediction or a model itself) [16, 41] while XDA enhances exploratory data analysis for understanding a data fact.

7 CONCLUSION

This paper advocates XDA, a concept that ships comprehensive and in-depth explainability toward EDA. XDA offers either causal or non-causal explanations for EDA outcomes, from both quantitative and qualitative perspectives. We have also presented the design of XINSIGHT, a production framework for XDA over databases. Experiments and human evaluations reveal that XINSIGHT manifests highly encouraging explanation capabilities. XPLAINER has been integrated into Microsoft Power BI.

REFERENCES

[1] 2022. Apply insights in Power BI to explain fluctuations in visuals. <https://docs.microsoft.com/en-us/power-bi/create-reports/desktop-insights>.

[2] 2022. Discover Insights Faster with Explain Data. https://help.tableau.com/current/pro/desktop/en-us/explain_data.htm.

[3] Firas Abuzaid, Peter Kraft, Sahaana Suri, Edward Gan, Eric Xu, Atul Shenoy, Asvin Ananthanarayanan, John Sheu, Erik Meijer, Xi Wu, et al. 2021. Diff: a relational interface for large-scale data explanation. *The VLDB Journal* 30, 1 (2021), 45–70.

[4] Rakesh Agrawal and Ramakrishnan Srikant. 1994. Fast Algorithms for Mining Association Rules in Large Databases. In *Proceedings of the 20th International Conference on Very Large Data Bases*. 487–499.

[5] Bryan Andrews, Peter Spirtes, and Gregory F Cooper. 2020. On the completeness of causal discovery in the presence of latent confounding with tiered background knowledge. In *International Conference on Artificial Intelligence and Statistics*. PMLR, 4002–4011.

[6] Nuno Antonio, Ana de Almeida, and Luis Nunes. 2019. Hotel booking demand datasets. *Data in brief* 22 (2019), 41–49.

[7] Peter Bailis, Edward Gan, Samuel Madden, Deepak Narayanan, Kexin Rong, and Sahaana Suri. 2017. Macrobase: Prioritizing attention in fast data. In *Proceedings of the 2017 ACM International Conference on Management of Data*. 541–556.

[8] Leopoldo Bertossi. 2020. Score-Based Explanations in Data Management and Machine Learning. In *International Conference on Scalable Uncertainty Management*. Springer, 17–31.

[9] Leopoldo Bertossi, Jordan Li, Maximilian Schleich, Dan Suciu, and Zografaoula Vagena. 2020. Causality-based explanation of classification outcomes. In *Proceedings of the Fourth International Workshop on Data Management for End-to-End Machine Learning*. 1–10.

[10] Michael Buckley. 2017. *Information and society*. MIT Press.

[11] Yiru Chen and Silu Huang. 2021. TSExplain: Surfacing Evolving Explanations for Time Series. In *Proceedings of the 2021 International Conference on Management of Data*. 2686–2690.

[12] Haoyue Dai, Rui Ding, Yuanyuan Jiang, Shi Han, and Dongmei Zhang. 2021. ML4C: Seeing Causality Through Latent Vicinity. *arXiv preprint arXiv:2110.00637* (2021).

[13] Rui Ding, Shi Han, Yong Xu, Haidong Zhang, and Dongmei Zhang. 2019. Quickinsights: Quick and automatic discovery of insights from multi-dimensional data. In *Proceedings of the 2019 International Conference on Management of Data*. 317–332.

[14] Rui Ding, Yanzhi Liu, Jingjing Tian, Zhouyu Fu, Shi Han, and Dongmei Zhang. 2020. Reliable and Efficient Anytime Skeleton Learning. In *Proceedings of the AAAI Conference on Artificial Intelligence*, Vol. 34. 10101–10109.

[15] Anna Fariha, Suman Nath, and Alexandra Meliou. 2020. Causality-guided adaptive interventional debugging. In *Proceedings of the 2020 ACM SIGMOD International Conference on Management of Data*. 431–446.

[16] Sainyam Galhotra, Romila Pradhan, and Babak Salimi. 2021. Explaining black-box algorithms using probabilistic contrastive counterfactuals. In *Proceedings of the 2021 International Conference on Management of Data*. 577–590.

[17] Boris Glavic, Alexandra Meliou, Sudeepa Roy, et al. 2021. Trends in Explanations: Understanding and Debugging Data-driven Systems. *Foundations and Trends® in Databases* 11, 3 (2021), 226–318.

[18] Joseph Y Halpern. 2016. *Actual causality*. MIT Press.

[19] Joseph Y Halpern and Judea Pearl. 2005. Causes and explanations: A structural-model approach. Part I: Causes. *The British journal for the philosophy of science* 56, 4 (2005), 843–887.

[20] Frank C Keil. 2006. Explanation and understanding. *Annu. Rev. Psychol.* 57 (2006), 227–254.

[21] Marc Lange. 2016. *Because Without Cause: Non-Causal Explanations In Science and Mathematics*. Oxford University Press.

[22] Po-Ming Law, Leo Yu-Ho Lo, Alex Endert, John Stasko, and Huamin Qu. 2021. Causal Perception in Question-Answering Systems. In *Proceedings of the 2021 CHI Conference on Human Factors in Computing Systems*. 1–15.

[23] Chenjie Li, Zhengjie Miao, Qitian Zeng, Boris Glavic, and Sudeepa Roy. 2021. Putting Things into Context: Rich Explanations for Query Answers using Join Graphs (extended version). *arXiv preprint arXiv:2103.15797* (2021).

[24] Pingchuan Ma, Rui Ding, Haoyue Dai, Yuanyuan Jiang, Shuai Wang, Shi Han, and Dongmei Zhang. 2022. ML4S: Learning Causal Skeleton from Vicinal Graphs. (2022).

[25] Pingchuan Ma, Rui Ding, Shi Han, and Dongmei Zhang. 2021. MetaInsight: Automatic Discovery of Structured Knowledge for Exploratory Data Analysis. In *Proceedings of the 2021 International Conference on Management of Data*. 1262–1274.

[26] Pingchuan Ma, Rui Ding, Shuai Wang, Shi Han, and Dongmei Zhang. 2022. XInsight: eXplainable Data Analysis Through The Lens of Causality. <https://doi.org/10.48550/ARXIV.2207.12718>

[27] Ahmed Mabrouk, Christophe Gonzales, Karine Jabet-Chevalier, and Eric Chojnacki. 2014. An efficient Bayesian network structure learning algorithm in the presence of deterministic relations. In *ECAI 2014*. IOS Press, 567–572.

[28] Alexandra Meliou, Wolfgang Gatterbauer, Joseph Y Halpern, Christoph Koch, Katherine F Moore, and Dan Suciu. 2010. Causality in databases. *IEEE Data Engineering Bulletin* 33, ARTICLE (2010), 59–67.

[29] Alexandra Meliou, Wolfgang Gatterbauer, Katherine F Moore, and Dan Suciu. 2010. The complexity of causality and responsibility for query answers and non-answers. *Proceedings of the VLDB Endowment* 4, 1 (2010), 34–45.

[30] Alexandra Meliou, Wolfgang Gatterbauer, Suman Nath, and Dan Suciu. 2011. Tracing data errors with view-conditioned causality. In *Proceedings of the 2011 ACM SIGMOD International Conference on Management of data*. 505–516.

[31] Alexandra Meliou, Sudeepa Roy, and Dan Suciu. 2014. Causality and explanations in databases. *Proceedings of the VLDB Endowment* 7, 13 (2014), 1715–1716.

[32] Zhengjie Miao, Qitian Zeng, Boris Glavic, and Sudeepa Roy. 2019. Going beyond provenance: Explaining query answers with pattern-based counterbalances. In *Proceedings of the 2019 International Conference on Management of Data*. 485–502.

[33] Tova Milo and Amit Shomech. 2020. Automating exploratory data analysis via machine learning: An overview. In *Proceedings of the 2020 ACM SIGMOD International Conference on Management of Data*. 2617–2622.

[34] Gregory L Murphy and Douglas L Medin. 1985. The role of theories in conceptual coherence. *Psychological review* 92, 3 (1985), 289.

[35] Judea Pearl. 2009. Causal inference in statistics: An overview. *Statistics Surveys* 3, none (2009), 96 – 146.

[36] Judea Pearl. 2009. *Causality*. Cambridge university press.

[37] Jonas Peters, Dominik Janzing, and Bernhard Schölkopf. 2011. Causal inference on discrete data using additive noise models. *IEEE Transactions on Pattern Analysis and Machine Intelligence* 33, 12 (2011), 2436–2450.

[38] Jonas Peters, Dominik Janzing, and Bernhard Schölkopf. 2017. *Elements of causal inference: foundations and learning algorithms*. The MIT Press.

[39] David L Poole and Alan K Mackworth. 2010. *Artificial Intelligence: foundations of computational agents*. Cambridge University Press.

[40] Mark Povich and Carl F Craver. 2018. Because without Cause: Non-Causal Explanations in Science and Mathematics.

[41] Romila Pradhan, Aditya Lahiri, Sainyam Galhotra, and Babak Salimi. 2022. Explainable AI: Foundations, Applications, Opportunities for Data Management Research. In *Proceedings of the 2022 International Conference on Management of Data*. 2452–2457.

[42] Sudeepa Roy and Dan Suciu. 2014. A formal approach to finding explanations for database queries. In *Proceedings of the 2014 ACM SIGMOD international conference on Management of data*. 1579–1590.

[43] Babak Salimi, Corey Cole, Dan RK Ports, and Dan Suciu. 2017. Zaliql: causal inference from observational data at scale. *Proceedings of the VLDB Endowment* 10, 12 (2017), 1957–1960.

[44] Babak Salimi, Harsh Parikh, Moe Kayali, Lise Getoor, Sudeepa Roy, and Dan Suciu. 2020. Causal relational learning. In *Proceedings of the 2020 ACM SIGMOD International Conference on Management of Data*. 241–256.

[45] Richard Scheines, Peter Spirtes, and Clark Glymour. 1991. A qualitative approach to causal modeling. In *Qualitative simulation modeling and analysis*. Springer, 72–97.

[46] Peter Spirtes, Clark N Glymour, Richard Scheines, and David Heckerman. 2000. *Causation, prediction, and search*. MIT press.

[47] Sofia Triantafillou and Ioannis Tsamardinos. 2015. Constraint-based causal discovery from multiple interventions over overlapping variable sets. *The Journal of Machine Learning Research* 16, 1 (2015), 2147–2205.

[48] David S Watson, Limor Gultchin, Ankur Taly, and Luciano Floridi. 2021. Local explanations via necessity and sufficiency: Unifying theory and practice. In *Uncertainty in Artificial Intelligence*. PMLR, 1382–1392.

[49] Eugene Wu and Samuel Madden. 2013. Scorpion: Explaining Away Outliers in Aggregate Queries. *Proceedings of the VLDB Endowment* 6, 8 (2013).

[50] Dong Young Yoon, Ning Niu, and Barzan Mozafari. 2016. Dbsherlock: A performance diagnostic tool for transactional databases. In *Proceedings of the 2016 International Conference on Management of Data*. 1599–1614.

[51] Kui Yu, Xianjie Guo, Lin Liu, Jiuyong Li, Hao Wang, Zhaolong Ling, and Xindong Wu. 2020. Causality-based feature selection: Methods and evaluations. *ACM Computing Surveys (CSUR)* 53, 5 (2020), 1–36.

[52] Jiji Zhang. 2008. On the completeness of orientation rules for causal discovery in the presence of latent confounders and selection bias. *Artificial Intelligence* 172, 16–17 (2008), 1873–1896.

8 SUPPLEMENTARY MATERIAL

8.1 Principle of Explainability under AVG and SUM

In AVG, we notice that $\text{AVG}_M(s_1) \approx \mathbb{E}(M | F = f_1)$ and $\text{AVG}_M(s_2) \approx \mathbb{E}(M | F = f_2)$ asymptotically. $\text{AVG}_M(s_1 \wedge X = x) \approx \mathbb{E}(M | F = f_1, X = x) = \mathbb{E}(M | F = f_1) = \text{AVG}_M(s_1)$. Similarly, $\text{AVG}_M(s_2 \wedge X = x) \approx \text{AVG}_M(s_1)$. Hence, $\Delta(D) \approx \Delta(D_{X=x})$.

In SUM, we notice that $\text{SUM} = \text{COUNT} \times \text{AVG}$ and $\text{COUNT}_M(s_1) = N \times P(F = f_1)$, $\text{COUNT}_M(s_2) = N \times P(F = f_2)$, where N is a constant indicating the number of rows in the data. Then, $\Delta = N(P(F = f_1)\mathbb{E}(M | F = f_1) - P(F = f_2)\mathbb{E}(M | F = f_2))$. $\Delta(D_{X=x}) = N(P(F = f_1, X = x)\mathbb{E}(M | F = f_1, X = x) - P(F = f_2, X = x)\mathbb{E}(M | F = f_2, X = x)) = N(P(F = f_1, X = x)\mathbb{E}(M | F = f_1) - P(F = f_2, X = x)\mathbb{E}(M | F = f_2))$.

8.2 Proof of Theorem. 3.1

LEMMA 8.2.1. *If $X \xrightarrow{\text{FD}} Y$, then $Y \not\perp\!\!\!\perp X$, and for any other variable set Z , $Z \perp\!\!\!\perp Y | X$.*

PROOF. Because $X \xrightarrow{\text{FD}} Y$, $P(Y | X) = I_{Y=f(X)}$. Since $|X|, |Y| > 1$, the following inequality holds.

$$P(XY) = P(X)P(Y | X) = P(X)I_{Y=f(X)} \neq P(X)P(Y) \quad (8)$$

Therefore, $Y \not\perp\!\!\!\perp X$. Given a variable set Z ,

$$\begin{aligned} P(YZ | X) &= \frac{P(XYZ)}{P(X)} \\ &= \frac{P(XZ)I_{Y=f(X)}}{P(X)} \\ &= P(Z | X)I_{Y=f(X)} \\ &= P(Z | X)P(Y | X) \end{aligned} \quad (9)$$

Therefore, $Z \perp\!\!\!\perp Y | X$. \square

LEMMA 8.2.2. *If $X \xrightarrow{\text{FD}} Y$ and $Z \perp\!\!\!\perp X | W$, then $Z \perp\!\!\!\perp Y | W$, where Z and W are two disjoint variable set other than X and Y .*

PROOF. Let $\pi_y = \{x | f(x) = y\}$. Therefore, $\{X \in \pi_y\} = \{Y = y\}$. Since $Z \perp\!\!\!\perp X | W$,

$$\begin{aligned} P(Y = y, Z | W) &= P(X \in \pi_y, Z | W) \\ &= P(X \in \pi_y | W)P(Z | W) \\ &= P(Y = y | W)P(Z | W) \end{aligned} \quad (10)$$

Therefore, $Z \perp\!\!\!\perp Y | W$. \square

LEMMA 8.2.3. *In a MAG G over variables $\{X_1, \dots, X_n\}$, if $X_1 \rightarrow X_2$ and no other edges connect X_2 with other vertices, when $X_2 \perp\!\!\!\perp M | U$ for any $M \in \{X_3, \dots, X_n\}$, $U \subset \{X_3, \dots, X_n\}$, $Y \notin U$, $X_1 \perp\!\!\!\perp Y | U$.*

PROOF. If $X_2 \perp\!\!\!\perp M | U$, according to the definition of m-separation, each path between X_2 and M satisfies one of the following two conditions: 1) there exists $X_p \rightarrow X_s \rightarrow X_q, X_p \leftarrow X_s \rightarrow X_q$, or $X_p \leftarrow X_s \leftarrow X_q$ where $X_s \in U$. 2) there exists $X_p \rightarrow X_s \leftarrow X_q$ where X_s or any of its descendants does not belong to U . Because $X_1 \notin U$, $X_1 \neq X_s$. For the first case, X_s blocks X_1 and M given that there is only one edge connecting to X_2 . For the second case, X_1

cannot be a collider, because $X_1 \rightarrow X_2$. Therefore, U also blocks X_1 and M on this path. In summary, $X_1 \perp\!\!\!\perp M | U$. \square

With above lemmas, now we prove Theorem. 3.1.

PROOF. We first construct a MAG G on the top of the skeleton, by adding an arrowhead from X_1 to Z (G_2). Because S_1 is learnt from $\{X_1, \dots, X_n\}$ where faithfulness assumption holds, this part is harmonious. For Z , there are two types of m-separation in G . Here, we prove that each types of m-separation satisfies GMP to data distribution P_V .

Type 1: $Z \perp\!\!\!\perp M | X_{j \neq 1} | X_1$

According to Lemma. 8.2.1, $X_1 \xrightarrow{\text{FD}} Z$ implies that $Z \perp\!\!\!\perp X_{j \neq 1} | X_1$.

Type 2: $Z \perp\!\!\!\perp M | X_j | U (j \neq 1, U \cap \{X_1, X_j\} = \emptyset)$

By Lemma. 8.2.3, $Z \perp\!\!\!\perp M | X_j | U$ implies that $X_1 \perp\!\!\!\perp M | X_j | U$. Because S_1 is harmonious, $X_1 \perp\!\!\!\perp M | X_j | U$ implies that $X_1 \perp\!\!\!\perp X_j | U$. According to Lemma. 8.2.2, $X_1 \xrightarrow{\text{FD}} Z$ and $X_1 \perp\!\!\!\perp X_j | U$ imply $Z \perp\!\!\!\perp X_j | U$.

Minimality is satisfied, since removing edge from X_1 to Z will make $X_1 \perp\!\!\!\perp Z$ which contradicts P_V . \square

8.3 Proof of Theorem. 3.2

PROOF. We prove Theorem. 3.2 by mathematical induction. In the sense, Alg. ?? returns a harmonious skeleton when G_{FD} has arbitrary number of non-root vertices. Denote the number of non-root vertices as $s \geq 0$.

Base Case. When $s = 0$, the skeleton is harmonious because all variables are under faithfulness assumptions.

Induction. Suppose the returned skeleton is harmonious for G_{FD} when $s = n$. Now we prove the skeleton is still harmonious when we add a vertex X' to a vertex set $\mathcal{X} \subseteq G_{\text{FD}}.V$. Denote the new FD-induced graph as G'_{FD} , the skeleton of G_{FD} as S , and the skeleton for G'_{FD} as S' . According to Alg. ??, S, S' share the same vertices and edges (except X'). Given that S is harmonious, S' can be decomposed into two subgraphs, i.e., S_1, S_2 , where $S_1 = S$ and S_2 corresponds to X' and one edge from X' to one of \mathcal{X} . Since $X'' \xrightarrow{\text{FD}} X'$, by Theorem. 3.1, S' is harmonious.

By the principle of mathematical induction, Theorem. 3.2 holds. \square

8.4 FCI Rules on FD-related Edges

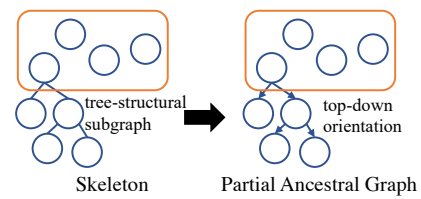


Figure 8: Orientation on tree-structural subgraph.

Since we only consider one-to-one and one-to-many FDs, FD-induced vertices only have at most one parent node in G_{FD} . Therefore, it forms tree-structural subgraphs in the skeleton starting from the root vertices of G_{FD} (e.g., the left-hand side skeleton shown in Fig. 8). Intuitively, it would be ideal if the orientation rules allow

us to orient the tree-structural subgraphs in a top-down manner (e.g., the right-hand side of Fig. 8). In particular, if there is an edge heading to the root node of the tree-structural subgraph, we can assign \rightarrow (\rightarrow is defined in Table 1) as the edge from the root node to its child vertices and propagate the directions to the leaf node by applying Rule 1 of FCI recursively.

DEFINITION 8.1 (RULE 1 OF FCI [52]). *If $X \rightarrow Y \rightarrow Z$ and X, Z are non-adjacent, then orient $Y \rightarrow Z$.⁶*

However, it is not necessarily attainable if we cannot identify the direction on the edge heading to the root node (i.e., Y in Def. 8.1). As a result, we cannot derive any directions on the subgraphs. That is, all edges on the subgraph are $\circ\circ$, which denote edges with unknown directions. Such ambiguous cases are surely undesirable in XDA scenarios.

8.5 ANM on FD-related Edges

We note that, from viewpoint of conditional independence, functional dependency does not imply causal directions in all cases. However, we present that the counterexamples of such cases (i.e., contrasting direction between causal relation and functional dependency) are very rare in practice, if at all possible. Recall the theorem of “Identifiability of discrete ANMs” in [38].

THEOREM 8.1. *Assume that a distribution $P_{X,Y}$ allows for an ANM $Y = f(X) + N_Y$ from X to Y and that either X or Y has finite support. $P_{X,Y}$ allows for an ANM from Y to X if and only if there exists a disjoint decomposition $\bigcup_{i=0}^l C_i = \text{supp}X$, such that the following conditions a), b), and c) are satisfied:*

a) *The C_i ’s are shifted versions of each other*

$$\forall i \exists d_i > 0 : C_i = C_0 + d_i \quad (11)$$

and f is piecewise constant: $f \mid C_i \equiv c_i \forall i$.

b) *The probability distributions on the C_i ’s are shifted and scaled versions of each other with the same shift constant as above: For $x \in C_i$, $P(X = x)$ satisfies*

$$P(X = x) = P(X = x - d_i) \cdot \frac{P(x \in C_i)}{P(x \in C_0)} \quad (12)$$

c) *The sets $c_i + \text{supp}N_Y := \{c_i + h : P(N_Y = h) > 0\}$ are disjoint sets.*

By condition c), since $N_Y = 0$ by functional dependency, $\nexists x_i \in C_i, x_j \in C_j$ s.t. $f(x_i) = f(x_j)$. In other word, X are decomposed by the value of $f(x)$ and each $c_i \in f(X)$ forms a disjoint subset C_i of X . To admit condition a), each C_i is a shifted version of others. Therefore, each C_i should at least have an equal cardinality. The above two conditions imply that each $y \in Y$ corresponds to equal size of $x \in X$. Consider the aforementioned example where Country $\xrightarrow{\text{FD}}$ Continent. To satisfy the condition, each continent must have equal number of countries. Furthermore, by condition b), the probability of a country x in continent c_i in the database can be exactly scaled by $\frac{P(x \in C_i)}{P(x \in C_0)}$ the probability of another shifted country $x - d_i$. The conditions together exhibits a very rare scenario. Therefore, we ignore such cases in practice.

⁶“*” is used as a wildcard symbol accepting either $\rightarrow, \leftrightarrow, \circ\circ$.

As consistent with [38], we consider it reasonable to infer that direction of ANM as causal. Therefore, we hypothesis that functional dependencies in G_{FD} intrinsically imply causal directions.

8.6 Proof of Proposition. 3.2

PROOF. Suppose there exists an optimal explanation P^* such that $\exists p_i \in P^*, \Delta_i \leq 0$. Let $P' = \{p \mid p \in P^*, \Delta_p > 0\}$ and Γ be the minimal contingency of P^* .

For SUM, since $\Delta(D_{P'}) \geq \Delta(D_{P^*})$, $\Delta(D) - \Delta(D_{\Gamma}) - \Delta(D_{P'}) < \Delta(D) - \Delta(D_{\Gamma}) - \Delta(D_{P^*}) \leq \epsilon$.

For homogeneous AVG,

$$\begin{aligned} \Delta(D - \Gamma - P') &= \frac{\sum_{p_i \in \{p_1, \dots, p_m\} - \Gamma - P'} a_i \Delta_i}{A_{D - \Gamma - P'}} \\ &< \frac{\sum_{p_i \in \{p_1, \dots, p_m\} - \Gamma - P^*} a_i \Delta_i}{A_{D - \Gamma - P^*}} \\ &= \Delta(D - \Gamma - P^*) \leq \epsilon \end{aligned} \quad (13)$$

Hence, Γ is also a valid contingency for P' . $\rho_{P'} \geq \rho_{P^*}$ and $|P'| < |P^*|$ contradict the fact that P^* is optimal. \square

8.7 Proof of Proposition. 3.3

PROOF. When there are more than one optimal explanations, let P' be the one with the smallest predicate size (i.e., $|P'|$) and Γ' be the corresponding minimal contingency. Otherwise, let P' and Γ' be the optimal explanation and corresponding minimal contingency, respectively. If $|P'| \geq |P^C|$, given that $\rho_{P'} \leq 1$ and $\rho_{P^C} = 1$, $\rho_{P'} - \sigma \rho_{P'} \leq \rho_{P^C} - \sigma \rho_{P^C}$. P^C is at least as optimal as P' . If $|P'| < |P^C|$, then let P'' be a predicate by replacing all non-canonical filters in P' with canonical ones. Then, $1 - d_{P''} \leq 1 - d_{P'} \leq \epsilon'$. Γ' is then a valid contingency for P'' . Therefore, $\rho_{P''} \geq \rho_{P'}$ and $|P''| = |P'|$. $\rho_{P''} - \sigma \rho_{P''} \geq \rho_{P'} - \sigma \rho_{P'}$. $P'' \subset P^C$ is at least as optimal as P' . In summary, there must exist an optimal explanation $P'' \subseteq P^C$. \square

8.8 Proof of Theorem. 3.3

PROOF. Let $m_k = \sum_{i=1}^k d_{p_i}$. According to the definition of canonical predicate, $1 - m_j \leq \epsilon' < 1 - m_{j-1}$. This inequality implies that $1 - (m_j - d_{p_j}) + d_{p_j} \leq \epsilon' < 1 - (m_j - d_{p_j})$. Since $\bar{P} \subset P^C$ and $d_{p_1} \leq \dots \leq d_{p_j}, d_{\bar{P}} \geq d_{p_j}$. The following inequalities hold.

$$\begin{aligned} \epsilon' &\geq 1 - (m_j - d_{\bar{P}}) - d_{\bar{P}} = 1 - d_P - d_{\bar{P}} \\ \epsilon' &< 1 - (m_j - d_{p_j}) \leq 1 - (m_j - d_{\bar{P}}) = 1 - d_P \end{aligned} \quad (14)$$

Since $1 - d_P - d_{\bar{P}} \leq \epsilon' < 1 - d_P$, Theorem. 3.3 holds. \square

8.9 Proof of Theorem. 3.4

PROOF. $\rho_P = \frac{1}{1 + \min(|\Gamma|_W)} \geq \frac{1}{1 + |\bar{P}|_W} = \frac{1}{1 + m_j - d_P}$. Furthermore, since $1 - d_P - d_{\Gamma} \leq \epsilon'$, $d_{\Gamma} \geq 1 - d_P - \epsilon'$ and $\rho_P \leq \frac{1}{2 - d_P - \epsilon'}$. Thus, we derive the lower and upper bounds of ρ_P . When assuming $d_P \ll m_j$ and $0 < m_j \leq 1$, $\frac{1}{1 + m_j - d_P} = \frac{1 + m_j + d_P}{(1 + m_j)^2 - d_P^2} \approx \frac{1 + m_j + d_P}{(1 + m_j)^2}$. The approximation error rate $E = \frac{\frac{1}{1 + m_j - d_P} - \frac{1 + m_j + d_P}{(1 + m_j)^2}}{\frac{1}{1 + m_j - d_P} - \frac{1}{(1 + m_j)^2}} = \frac{d_P^2}{(1 + m_j)^2} < \frac{m_j^2}{(1 + m_j)^2} \leq 0.25$. \square

8.10 Proof of Proposition. 3.4

To prove Proposition. 3.4, we first introduce the following notations and propositions.

Notations. Given WHY QUERY Δ and corresponding sibling subspaces s_1, s_2 , let x_i, y_i be $agg_M(D_{s_1 \cap p_i})$ and $agg_M(D_{s_2 \cap p_i})$, respectively. We also let a_i, b_i be $|D_{s_1 \cap p_i}|$ and $|D_{s_2 \cap p_i}|$ denoting the rows of $D_{s_1 \cap p_i}$ and $D_{s_2 \cap p_i}$, respectively, and A_D, B_D be $|D_{s_1}|$ and $|D_{s_2}|$. Then, it is obvious that $\Delta(D_{p_i}) = x_i - y_i$ and we use Δ_i as a shorthand for $\Delta(D_{p_i})$. For AVG and $\Delta(D_P) = \sum_{p_i \in P} \Delta_i$, $\Delta(D)$ can be represented in the form of $\sum_1^m \left(\frac{a_i x_i}{A_D} - \frac{b_i y_i}{B_D} \right)$.

PROPOSITION 8.1. *If a pair of sibling subspaces are homogeneous on X , then $\frac{a_1}{b_1} = \dots = \frac{a_m}{b_m}$.*

PROOF. For homogeneous AVG, X, F are m-separated given B . Hence, $X \perp\!\!\!\perp F \mid B$ and $P(X, F \mid B) = P(X \mid B)P(F \mid B)$. Recall that $a_i = P(X = x_i, F = f_1 \mid B = b)$ and $b_i = P(X = x_i, F = f_2 \mid B = b)$. We have $\frac{a_i}{b_i} = \frac{P(F=f_1|B=b)}{P(F=f_2|B=b)}$ which is a constant and invariant with respect to i . \square

PROPOSITION 8.2. *If P_1 and P_2 are two disjoint predicates on the same attribute, for homogeneous AVG, $\Delta(D_{P_1} + D_{P_2}) < \Delta(D_{P_1}) + \Delta(D_{P_2})$.*

PROOF. For homogeneous AVG, $\Delta(D_{P_1}) = \frac{\sum_{p_i \in P_1} a_i \Delta_i}{A_{P_1}}$, $\Delta(D_{P_2}) = \frac{\sum_{p_i \in P_2} a_i \Delta_i}{A_{P_2}}$ and $\Delta(D_{P_1} + D_{P_2}) = \frac{\sum_{p_i \in P_1 \cup P_2} a_i \Delta_i}{A_{P_1 \cup P_2}}$. Also, $A_{P_1 \cup P_2} = A_{P_1} + A_{P_2}$. Hence, $A_{P_1} < A_{P_1 \cup P_2}$ and $A_{P_2} < A_{P_1 \cup P_2}$. Therefore,

$$\begin{aligned} \Delta(D_{P_1}) + \Delta(D_{P_2}) &= \frac{\sum_{p_i \in P_1} a_i \Delta_i}{A_{P_1}} + \frac{\sum_{p_i \in P_2} a_i \Delta_i}{A_{P_2}} \\ &> \frac{\sum_{p_i \in P_1} a_i \Delta_i}{A_{P_1 \cup P_2}} + \frac{\sum_{p_i \in P_2} a_i \Delta_i}{A_{P_1 \cup P_2}} \quad (15) \\ &= \frac{\sum_{p_i \in P_1 \cup P_2} a_i \Delta_i}{A_{P_1 \cup P_2}} \\ &= \Delta(D_{P_1} + D_{P_2}) \end{aligned}$$

\square

Now, we prove Proposition. 3.4.

PROOF.

$$\begin{aligned} \Delta_{D_P - D_{P_j}} &= \frac{\sum_{p_i \in P} a_i \Delta_i - a_j \Delta_j}{A_{D - P_j}} \\ &= \frac{\sum_{p_i \in P} a_i \Delta_i - a_j \Delta_j}{A_D - a_j} \quad (16) \\ &< \frac{\sum_{p_i \in P} a_i \Delta_i}{A_D} \\ &= \Delta_{D_P} \end{aligned}$$

The inequality in the above equation is true because $\frac{A}{B} < \frac{C}{D}$ implies $\frac{A-C}{B-D} < \frac{A}{B}$ where A, B, C, D are positive and $A > C, B > D$. \square

8.11 Generating Synthetic Data

③ Synthetic Data A (SYN-A). We use Erdős-Rényi model, a well-established random graph model, to synthesize random causal graphs of different scales and to produce datasets via forward sampling [39]. To simulate causally insufficient systems, we mask 5%

variables at random and return the corresponding PAG (Partial Ancestral Graph) as the ground truth. On randomly-selected 85% of variables, we construct conditional probability tables based on a Dirichlet prior; the remaining 15% of variables are mandated to be functionally dependent on their parent node. Afterwards, these functional dependencies are employed to build FD-induced graphs.

③ Synthetic Data B (SYN-B). In particular, we design a data generating process with three variables X, Y, Z , where X is a binary variable, Y is a categorical variable, and Z is a numerical variable. Different values in X first impact Y and then Y 's values further impact Z . When Y 's realizations are equal to some specific values (i.e., $Y \in \{y_1, \dots, y_k\}$), Z would be sampled from a Gaussian distribution with a higher mean μ^* ; otherwise, Z is sampled from another Gaussian distribution with a lower mean $\mu < \mu^*$. Note that the higher k , the harder XPLAINER (and other tools) to comprehensively identify all filters to form the correct explanation. As a result, given different X , the aggregated result of Z differs. Recall Def. 2.1 where X and Z form the context and the target of a WHY QUERY. Then, we seek to extract the explanation from Y and the way Y impacts Z specified in the data generating process (i.e., $Y = y_1 \vee \dots \vee Y = y_k$) constitutes the ground truth of this WHY QUERY. We concretize the above data generating process with different parameters (e.g., cardinality and conditional probability table of Y and conditional distributions of Z) and yield 18 datasets of different difficulties. By default, we generate SYN-B datasets with 10,000 rows; the variable Y contains ten values, three of which would trigger abnormal Z (i.e., $Z \sim \mathcal{N}(\mu^*, 10)$, $\mu^* = 60$) while the others would produce normal $Z \sim \mathcal{N}(\mu, 10)$, $\mu = 10$. The parameters are on a par with the configuration in Scorpion.